https://rbgeomorfologia.org.br/
ISSN 2236-5664

Revista Brasileira de Geomorfologia

v. 25, nº 2 (2024)

http://dx.doi.org/10.20502/rbg.v24i2.2451

Research Article

Soil erosion vulnerability in Brazilian semiarid

Vulnerabilidade à erosão do solo no semiárido brasileiro

Vilaneide Lopes Costa de Oliveira [1], Jessica Neves de Carvalho [2], Luiz Antonio Cestaro [3] e José João Lelis Leal de Souza [4]

[1] Universidade Federal do Rio Grande do Norte, Departamento de Geografia, Natal, Brasil. vilaneide_oliveira@yahoo.com.br
ORCID: https://orcid.org/0000-0001-8962-0692
[2] Universidade Federal de Viçosa, Departamento de Solos, Viçosa, Brasil. E-mail. jessica.n.carvalho@ufv.br
ORCID: https://orcid.org/0000-0002-4675-732X
[3] Universidade Federal do Rio Grande do Norte, Departamento de Geografia, Natal, Brasil. luiz.cestaro@ufrn.br
ORCID: http://orcid.org/0000-0003-0430-8566
[4] Universidade Federal de Viçosa, Departamento de Solos, Viçosa, Brasil. E-mail. jjlelis@ufv.br
ORCID: https://orcid.org/0000-0003-4670-6626

Received: 19/07/2023; Accepted: 20/03/2024; Published: 03/07/2024

Abstract: Soil erosion is one of the most dangerous impacts of climate change and anthropic disturbance in drylands. Its control and reduction of soil and nutrient loss are essential to maintaining terrestrial ecosystems. Rare studies present data about soil fragility in the Brazilian semiarid. This study aimed to measure soil resistance to erosion. Ten soil profiles were described and classified to represent vegetation cover and geological diversity. The study area encompasses the Seridó region, one of the driest regions in Brazil. The water-stable aggregates (WSA) content is highly variable, regardless of the equivalent diameter of the aggregates. The lowest levels of WSA were recorded by Arenosol and A and E horizons of Solonetz. Plinthosol and argic horizon of Solonetz and Luvisol recorded the lowest levels of soil loss. Large and fine aggregates presented different stability mechanisms. Vegetation cover, clay, and sand contents intermediate the stability of aggregates larger than 1 mm. Soil reactivity, Al^{3+} content, and altitude are important for aggregates smaller than 1 mm. Conservation practices that favor coverage and maintenance of soil moisture and organic residues should be induced by the government and applied by small rural producers to minimize human environmental effects.

Keywords: Dry forest; Soil fragility; Desertification; Caatinga; Drylands

Resumo: A erosão do solo é um dos impactos mais danosos ocasionado pelas mudanças climáticas e pela ação antrópica em terras secas. Seu controle e redução da perda de solo e nutrientes são essenciais para a manutenção dos ecossistemas terrestres. São raros os estudos que apresentam dados sobre a fragilidade do solo no semiárido brasileiro. Este trabalho teve como objetivo medir a resistência do solo à erosão. Dez perfis de solo foram descritos e classificados para representar a cobertura vegetal e a diversidade geológica. A área de estudo abrange a região Serió Poioguar, uma das mais secas do Brasil. O teor de agregados estáveis em água (WSA) é altamente variável, independentemente do diâmetro equivalente dos agregados. Os menores níveis de WSA foram registrados pelo Neossolo Quartzarênico e horizontes A e E do Planossolo. O Plintossolo e o horizonte Bt do Planossolo e Luvissolo registraram os menores níveis de perda de solo. Os agregados de maior e menor tamanho apresentaram diferentes mecanismos de estabilidade. A cobertura vegetal, teores de argila e areia intermediam a estabilidade de agregados maiores que 1 mm. A reatividade do solo, o teor de Al^{3+} e a altitude são importantes para agregados menores que 1 mm. Práticas conservacionistas que favoreçam a cobertura e manutenção da umidade do solo e dos resíduos orgânicos devem ser induzidas pelo poder público e aplicadas pelos pequenos produtores rurais para minimizar os efeitos antrópicos no meio ambiente.

Palavras-chave: Floresta seca; Fragilidade do solo; Desertificação; Caatinga; Terras secas

1. Introduction

Soils are complex mixtures of minerals, water, air, and organic matter and host a large diversity of organisms that interfere in several biogeochemical cycles (LAL, 2018). Although its relevance in sustaining life, it is estimated that by 2050 around 1.5 million km^2 of soil will be lost by erosion (FAO, 2019). Studies suggest that half of all crop and pasture areas in Brazil are degraded due to soil erosion (EMBRAPA, 2002).

Loss of soil favors CO_2 emission into the atmosphere (LAL, 2006, 2018; OLSON *et al.*, 2016), loss of nutrients (CHARTIER et al., 2013; TRAORÉ et al., 2015; WOLKA et al., 2021), pollution, and silting of rivers and reservoirs (BAKKER *et al.*, 2005), decrease in the ability to infiltrate and retain water in soils(SANTOS et al., 2016), destruction of natural habitats (PRINCE *et al.*, 2018), and acceleration of the desertification process (SOUZA et al., 2009; FAO, 2017; IPCC, 2019).

Liquid water is the major erosive agent in tropical areas, and its erosivity is conditioned by the intensity of rainfall, gravitational potential, and terrain slope (FAO, 2019b). Soil properties also mediate erosion. Content of soil organic matter (SIX et al., 2004; WUDDIVIRA and CAMPS-ROACH, 2007; BLAUD et al., 2014), shrink-swell process (DIEL et al., 2019), tri and divalent cations contents (ROWLEY et al., 2018), bioturbation (SCHAEFER, 2001; BLAUD et al., 2014; LEHMANN and RILLIG, 2015), total porosity, and structure (TOTSCHE *et al.*, 2018a) are the main features that influence soil resistance to erosion.

The low density of vegetation cover (WANG et al., 2016; Leite et al., 2018) and spatio-temporal rainfall variability (SANTOS et al., 2011, 2016; SANTOS et al., 2018) induce higher erosion rates in semiarid environments compared to wet tropical regions. The Brazilian semiarid region hosts more than 54 million inhabitants (IBGE, 2023), comprising one of the most populated semiarid regions on the planet (MARENGO, 2008). Annual precipitation is below 800 mm, and potential evapotranspiration is up to four times greater than precipitation (KAYANO AND ANDREOLI, 2009). A shrub deciduous vegetation cover is dominant and usually composed of thorny, cactus, and bromeliad plants (QUEIROZ *et al.*, 2018). Leptosols, Regosols, and Luvisols are the main soil groups and reflect incipient weathering and pedogenesis (ARAÚJO et al., 2017).

The studies on erosion in the Brazilian semiarid region show discrepant results (SAMPAIO, 2008; XAVIER, 2016, 2021). For example, a straight relation between rainfall and soil erosion is indicated in some studies (dos SANTOS, 2009; LOBATO et al., 2009; PALÁCIO et al., 2016) and not confirmed in others (BORGES NETO et al., 2023; LEITE et al., 2018), suggesting a lack of knowledge about the complexity of the process. Knowledge of the mechanisms that retard the erosive process is fundamental for planning and elaborating soil conservation projects. Therefore, this study aimed to measure soil erosion fragility by water and eolian erosion processes in different classes in the Brazilian semiarid region. Here we included those soil groups which express more than 90% of the Brazilian semiarid total area: Luvisols, Leptosolos, Arenosols, Ferralsols, Cambisols, Solonetzs, and Plinthosols (Santos et al., 2011). We hypothesize that aggregate resistance to erosion significantly differs between soil groups according to their texture and reactivity.

2. Study area

The study area encompasses the Seridó Potiguar region in Rio Grande do Norte state. It has a total area of approximately 9,374 km^2 and particular landscape diversity. The altitude varies between 150 m, in valleys, and 750 m, in plateaus associated with Cenozoic sandstone. Seridó Potiguar is one of the driest regions in Brazil. Areas below 400 m of altitudes have mean precipitation of 500 mm year^{-1}, concentrated between January and May, and evapotranspiration is up to four times higher than precipitation. The average temperature is above 30 °C in all months of the year (KAYANO and ANDREOLI, 2009). On the other hand, areas at higher altitudes have peculiar climatic dynamics derived from a local type of "valley-mountain" circulation, thus favoring the occurrence of orographic rains, fog, and a high number of springs. The mean temperature in highlands is up to 5 °C lower than lowlands (LUCENA *et al.*, 2022).

Leptosols (17% of the total area), Luvisols (11%), and Regosols (2%) occur in pediment surfaces partially eroded and associated with horst–graben systems (XAVIER *et al.*, 2016). These soils occur between 350 and 400 m and are developed from Proterozoic gneiss and schists (ANGELIM et al., 2006; SANTOS et al., 2011). Planosols (10%), Vertisols (>1%), and Fluvisols (>1%) occur on alluvial plains and terraces, between 160 and 250 m, over Cenozoic sediments. These soils are dominantly loamy, shallow (<1 m deep), eutrophic, and have low organic carbon content (RÜCKAMP et al., 2010; GIONGO et al., 2011; MENEZES et al., 2012; FERREIRA et al., 2018).

Shrubs, 3 to 9 m height-trees that shed their leaves seasonally, cacti, and arid-adapted grasses, such as *Anadenanthera colubrine*, and *Cenostigma piramydale*, cover the lowlands (AMORIM et al., 2005; ALVES et al., 2011; APG, 2016).

Ferralsols (26%), Arenosols (9%), and Plinthosols (>1%) cover plateaus, between 350 and 700 m, derived from Cenozoic sandstones. These soils are dominantly acidic, deep, dystrophic, and have organic carbon content higher than 1% (ARAÚJO et al., 2017). Semideciduos forest cover the highlands and are composed by non-drought species, as *Bowdichia nitida, Manilkara bidentata, Tapirira guianensis, Myrciaria cauliflora Harpochilus neesianus*, *Ruellia geminiflora*, *Schinopsis brasiliensis*, and *Mandevilla dardanoi* (GARIGLIO *et al*., 2010).

Extensive livestock and agriculture have been practiced since European colonization in the 18th century. Between 1940 and 1970, scheelite mining took place in open pit mines. A prolonged drought between 1964 and 1970 and the low technical production level led to crises in these productive sectors (MARENGO, 2008). The population density is 35.20 hab km² (IBGE, 2022), one of the highest among the semiarid regions of the planet.

3. Material and Methods

3.1 Sampling and soil analysis

Ten soil profiles were described to represent the geomorphological and geological diversity of the study area (Figure 1). Diagnostic horizons, attributes, and properties were identified according to the morphological description (color, texture, structure, consistency, thickness, roots, and pores). At each pedon, soil samples were collected on each horizon, from the surface down to the lithic contact. For deeper soils, a 200-cm control section was used. All soil profiles were classified according to the World Reference Base for soil resources (IUSS WORKING GROUP WRB, 2015). Pedons also were classified according to the SiBCS (SANTOS *et al*., 2018).

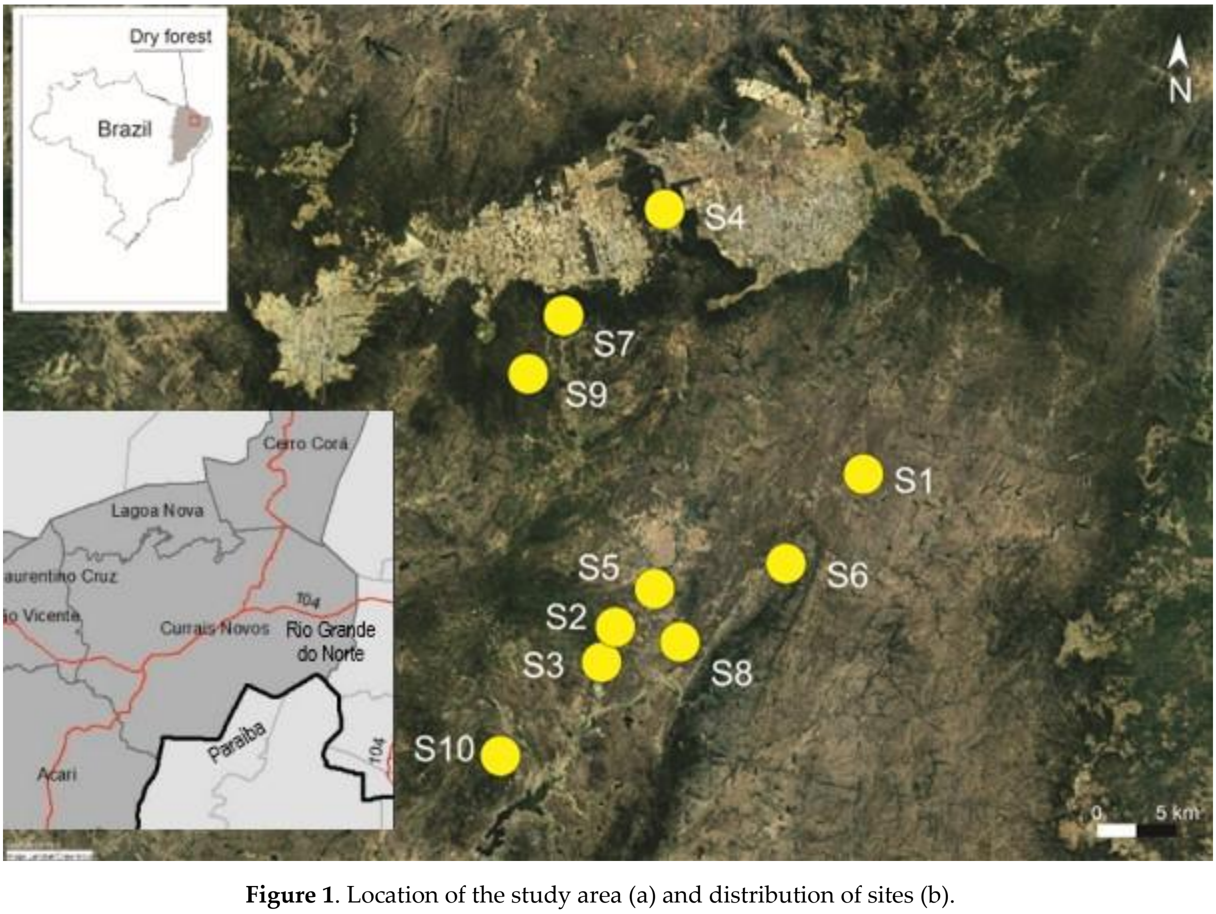

Figure 1. Location of the study area (a) and distribution of sites (b).

Biomass and primary productivity were estimated by Landsat surface reflectance-derived soil adjusted vegetation index (SAVI). The SAVI derives from Landsat 4–5 Thematic Mapper (TM), Landsat 7 Enhanced

Thematic Mapper Plus (ETM+), and Landsat 8 Operational Land Imager (OLI)/Thermal Infrared Sensor (TIRS) scenes that can be processed to Landsat Level-2 Surface Reflectance products. Landsat Surface Reflectance-derived SAVI is calculated as a ratio between the R and NIR values with a soil brightness correction factor (L) defined as 0.5 to accommodate most land cover types. SAVI is used to correct Normalized Difference Vegetation Index (NDVI) for the influence of soil brightness in areas where vegetative cover is low.

According to methods established for tropical soils, samples were air-dried and sieved through a 2.0-mm sieve before physical and chemical analysis (TEIXEIRA et al., 2017). Sand, silt, and clay content were determined by the pipette method after dispersion with 0.1 mol L^{-1} NaOH. Textural classes were identified according to WRB (IUSS WORKING GROUP WRB, 2014). Soil pH was measured with a glass electrode in a 1:2.5 suspension v/v soil and deionized water (pH H_2O). The content of Ca^{2+}, Mg^{2+}, and exchangeable acidity (H+Al) were determined in an unbuffered 1 mol L^{-1} KCl extract. The potential acidity (PA) at pH 7.0 was determined in a 1 M ammonium acetate solution at pH 7. Exchangeable K^+ and Na^+ were determined by flame photometry after Melhich-1 extraction. From these results, we calculated the sum of bases (BS), base saturation (V), aluminum saturation (m), equivalent cation exchange capacity (ECEC), and total cation exchange capacity (CEC).

Available phosphorus content (P_M) was determined by photocolorimetry after Mehlich-1 extraction. The soil organic carbon (SOC) was determined by wet combustion (YEOMANS and BREMNER, 1988). Total nitrogen (N) was determined by the Kjeldahl method and titration (TEIXEIRA *et al.*, 2017b). The carbon to nitrogen ratio (C/N) was calculated on a mass basis. The P adsorption capacity of the soil (P_{REM}) was determined after stirring 2.5 g of soil in 0.01 mol L^{-1} $CaCl_2$ containing 60 mg of P L^{-1} for 1 hour. The suspension was filtered, and the remaining P in solution (P_{REM}) was determined by photocolorimetry. The higher the value of P_{REM}, the lower is the affinity of soils for the P in the solution. Texture and chemical analysis were executed in three aliquots and results have a coefficient of variation below 10%.

Undisturbed samples were collected using a metallic cylinder of 100 cm^3 in the surface and subsurface horizons of each soil group to determine soil density and water retention capacity (TEIXEIRA et al., 2017). Bulk density was calculated as the ratio between the mass of the samples after heating at 105 °C for 48 h - discounting the mass of the metallic cylinder - and the volume of each cylinder measured by pachymeter. Particle density was measured by weighing 20 g of soil after drying at 105 °C, then dividing that mass by the volume of the particles, measured by a volumetric flask and alcohol. Water retention was measured at matric potentials of -6, -10, -30, -60, -100, -300, -1500 kPa using a Richards' pressure plate apparatus. Total porosity was calculated using the formula: Total porosity=(1- Bulk density/Particle density). Water retained in the potential of -1500 kPa was considered non-available water. Available water was calculated as the difference between water retained in potentials of -30 and -1500 kPa. Three replicates were sampled for each horizon. Soil organic carbon and total nitrogen stocks were calculated using total organic content, sampling depth, and bulk density: Stock (kg m^{-2}) = bulk density (kg dm^{-3}) x total organic carbon (or total nitrogen) content (%) x depth (dm) (FIDALGO *et al.*, 2007).

3.2 Ped stability analysis and statistical procedures

Undisturbed samples of aggregates with an equivalent diameter greater than 10 cm were collected in all horizons. Aggregate stability was determined by wet and dry sieving apparatus according to traditional methodologies (TEIXEIRA et al., 2017). Each soil sieving stack consisted of 4 sieves ranging in size from 4 to 0.25 mm. Aggregate stability was expressed using percentage water stable aggregates (WSA), and mean weight diameter (MWD). MWD was calculated by the formula (HAYNES, 1993):

$$MWD = \Sigma_{i=1}^{n} F_i . D_i$$

where Fi is the corrected mass proportion of stable aggregate fraction i in the total 0.25–10 mm aggregate and Di is the mean diameter of stable aggregate fraction i. Three aliquots of 25 g each of air-dried aggregates retained on a 2 mm sieve were used for determinations.

Descriptive statistics were performed on water-stable aggregates. One-way analysis of variation (ANOVA)was used to evaluate statistical difference of aggregate stability. Tukey's HSD test was used to determine the significance level ($p < 0.05$). The Pearson correlation between the water stable aggregates content, the properties of each soil horizon, SAVI, slope, and altitude was calculated. Properties significantly correlated ($p<0.05$) with aggregate indices were incorporated into a multiple linear regression model. The equation with the highest adjusted coefficient of determination and lowest residual was selected.

4. Results

Two Solonetz were described on fluvial terraces at the lowest altitude of the study area (Table 1). A Luvisol was described on a pediment surface derived from gneiss. Two Leptosols and two Regosol were described in backslope. They are derived from granites and granitoids. A Plinthosol was described in a plateau shoulder. An Arenosol and an Acrisol, derived from sandstone, were described in a summit. Dry forest species dominated in all profiles, except in the plateaus. Fragments of semideciduous forest were found over Acrisol and Arenosol.

Table 1. Site description of the soil profiles.

Soil profile	SiBCS	WRB	Altitude (m)	Site description	Coordinates *
Lowlands in pediment plain					
1	NEOSSOLO LITÓLICO Eutrófico fragmentário	Eutric Leptosol (Loamic, Humic, Yermic, Raptic)	387	Soil described in a middle third slope of the Borborema plateau. Surface has 30° of slope. Well-drained soil, with strong laminar erosion and derived from gneiss. Quartz and feldspar occur as gravel in all soil profile. *Commiphora leptophloeos*, *Croton blanchetianus,* and *Jatropha mollissima* dominate a dry forest fragment. Soil is covered by sparse litter.	6.21552°S 36.42868°W
2	LUVISSOLO CRÔMICO Órtico típico	Leptic Abruptic Luvisol (Clayic, Cutanic, Differentic, Hypereutric, Ochric, Raptic)	367	Soil described in a pediment plain. Surface has 10° of slope. Well-drained soil, with strong laminar erosion and derived from gneiss. Quartz and feldspar occur as gravel in all soil profile. Sparse grasses and no litter on soil. *Anadenanthera colubrine*, and *Cenostigma piramydale* dominate a dry forest fragment. Soil is covered by sparse litter. Clay coatings were identified in the B horizon.	6.23568°S 36.47816°W
3	NEOSSOLO REGOLÍTICO Eutrófico típico	Hypereutric Regosol (Loamic,	395	Soil described in an inselberg. Surface has 40° of slope. Well-drained soil, with strong laminar	6.18171°S 36.527780°W

		Ochric, Yermic, Raptic)		erosion and derived from granite. Quartz and feldspar occur as gravel in all soil profile. Sparse grasses and no litter on soil. *Commiphora leptophloeos*, *Croton blanchetianus,* and *Jatropha mollissima* dominate a dry forest fragment.	
5	PLANOSSOLO NÁTRICO Órtico dúrico	Stagnic Abruptic Solonetz (Clayic, Columnic, Cutanic, Differentic, Ochric, Magnesic, Hypernatric, Raptic)	300	Soil described in a stream terrace. Surface has 2° of slope. Poor-drained soil, with slight laminar erosion and derived from alluvial sediments. Dominance of *Cenostigma piramydale*. Litter covers the soil surface, and bioturbation is limited to the first horizon.	6.338335°S 36.529220°W
7	NEOSSOLO LITÓLICO Eutrófico típico	Hypereutric Regosol (Loamic, Ochric, Yermic)	427	Soil described in a should of a slope. Surface has 40° of slope. Well-drained soil, with strong laminar erosion and derived from granite. Quartz and feldspar occur as gravel in all soil profile. Sparse grasses and no litter on soil. *Commiphora leptophloeos*, *Croton blanchetianus,* and *Jatropha mollissima* dominate a dry forest fragment.	6.1461697°S 36.58432°W
8	PLANOSSOLO NÁTRICO Órtico típico	Stagnic Solonetz (Albic, Loamic, Ochric, Magnesic, Hypernatric, Raptic)	300	Soil described in a stream terrace. Surface has 2° of slope. Poor-drained soil, with slight laminar erosion and derived from alluvial sediments. Dominance of *Cenostigma piramydale*. Litter covers the soil surface, and bioturbation is limited to the first horizon.	6.33622897°S 36.525395°W

9	NEOSSOLO LITÓLICO Eutrófico típico	Eutric Leptosol (Loamic, Ochric, Yermic)	447	Soil described in a middle third slope of the Borborema plateau. Surface has 30° of slope. Well-drained soil, with strong laminar erosion and derived from gneiss. Quartz and feldspar occur as gravel in all soil profile. *Commiphora leptophloeos*, *Croton blanchetianus*, and *Jatropha mollissima* dominate a dry forest fragment. Soil is covered by sparse litter.	6.19636564°S 36.603682°W
Highlands in plateau					
4	ARGISSOLO AMARELO Distrófico típico	Xanthic Acrisol (Clayic, Hyperdystric, Ochric, Raptic)	680	Soil described in a plateau. Surface has 5° of slope. Well-drained soil, with slight laminar erosion and derived from sandstone. *Harpochilus neesianus*, *Ruellia geminiflora*, *Schinopsis brasiliensis*, and *Mandevilla dardanoi* dominate a semideciduous forest fragment. Litter covers the soil surface, and bioturbation is intense. A 10 cm-depth surface horizon buries soil.	6.088025°S 36.527140°W
6	NEOSSOLO QUARTZARÊNICO Órtico leptico	Hypereutric Arenosol (Ochric)	412	Soil described in a plateau. Surface has 5° of slope. Well-drained soil, with slight laminar erosion and derived from quartzite. *Harpochilus neesianus*, *Ruellia geminiflora*, *Schinopsis brasiliensis*, and *Mandevilla dardanoi* dominate a semideciduous forest fragment. Litter covers the soil surface, and bioturbation is intense.	6.263237°S 36.451164°W
10	PLINTOSSOLO HÁPLICO Eutrófico petroplínticos	Geric Plinthosol (Clayic, Eutric, Ochric, Raptic)	675	Soil described in a scarp of a plateau. Surface has 30° of slope. Well-drained soil, with strong laminar erosion and derived from petroferric layer. Iron nodules occur as gravel in all soil profile. *Commiphora leptophloeos*, *Croton*	6.39039298°S 36.603681°W

	blanchetianus, and *Jatropha mollissima* dominate a dry forest fragment. Soil is covered by sparse litter.

* World Geographic System, SIRGAS 2000 Datum.

Soil thickness varied between 20 and 200 cm (Table 2). The A-C and A-B sequences were recurrent. The transition between horizons varied between abrupt and diffuse, being predominantly smooth and clear. The dominant structures are of moderate grade, fine to medium size, and subangular and angular block types. Roots are dominantly common, and in general, there is a decrease in the quantity of roots with increasing soil depth. Pores are predominantly fine and common.

Table 2. Morphological soil properties.

Horizon	Depth (cm)	Boundary (distinctness, topography)	Structure (grade, size, type)	Moist color	Consistence (dry, moist, wetter, cementation)	Redoximorphic features (kind, quantity, size, contrast, state, hardness, boundary)	Nodule color	Roots (quantity, size)	Pores (quantity, size)
Lowlands in pediment plain									
S1 – Eutric Leptosol (Loamic, Humic, Yermic, Raptic)/ NEOSSOLO LITÓLICO Eutrófico fragmentário									
A	0-7	C-S	2, f/m, sbk	7.5YR 3/1	S, FR, po, so, NC	-	-	2, vf	2, f/m
Cr	0-25	C-S	1, m, sbk	10YR 3/6	S, FR, ps, ss, NC	-	-	1, vf	2, vf/f
R	25+	-	-	-	-	-	-	-	-
S2 –Leptic Abruptic Luvisol (Clayic, Cutanic, Differentic, Hypereutric, Ochric, Raptic)/ LUVISSOLO CRÔMICO Órtico típico									
A	0-30	C-S	2, m/co, sbk	10YR 3/2	SH, FR, ps, NC	-	-	1, vf	2, f
Bt	30-47	C-S	2, co, sbk	7.5 YR 3/4	SH, FR, vp, vs, NC	-	-	1, vf	1, f/m
Cr	47-70	C-S	0, -, m	10YR4/6	HA, VH, p-vp, vs, NC	-	-	1, m	2, f
R	70+	-	-	-	-	-	-	-	-
S3 - Hypereutric Regosol (Loamic, Ochric, Yermic, Raptic)/ NEOSSOLO REGOLÍTICO Eutrófico típico									
A	0-65	C-S	2, m/co, sbk	7.5 YR 3/2	HA, FR, p, s, NC	-	-	1, vf/f	3, f/m/co
Cr	65-112	G-S	0, -, m	10 YR 3/6	HA, FR, po, so, NC	-	-	1, vf/m	1, vf
R	112+	-	-	-	-	-	-	-	-
S5 - Stagnic Abruptic Solonetz (Clayic, Columnic, Cutanic, Differentic, Ochric, Magnesic, Hypernatric, Raptic)/ PLANOSSOLO NÁTRICO Órtico dúrico									
An1	0-10	C-S	2, f/m, sbk	10 YR 3/4	SH, FR, po, so, NC	-	-	2, vf/f	3, f/m
An2	10-12	A-S	1, f/m, sbk	10 YR 5/8	SH, FR, po, so, NC	-	-	1, m/co	3, f/m/co
Btnv1	12-48	C-S	3, vc, pr/cpr	10 YR 2/1	VH, VFR, vp, vs, NC	F3M,f, 2, F, D, I, C	10YR 4/6	1, m	1, vf/f

Btnv2	48-115+	-	3, vc, pr	10YR 3/4	VH-EH, FR, ps, ss, NC	F3M, f, 2, F, D, I, C	10YR 3/6	absent	1, f
S7 - Hypereutric Regosol (Loamic, Ochric, Yermic)/ NEOSSOLO LITÓLICO Eutrófico típico									
A	0-19	G-S	2, f/m, sbk	2.5Y 3/1	FR, po, ss, NC	-	-	2, vf/f/m	3, f/m/co
AC	19-45	G-W	1, m, sbk	2.5Y 3/2	FR, ps, s, NC	-	-	3, vf/f	2, f/m
R	45+	-	-	-	-				
S8 - Stagnic Solonetz (Albic, Loamic, Ochric, Magnesic, Hypernatric, Raptic)/ PLANOSSOLO NÁTRICO Órtico típico									
A	0-10	C-S	2, f/m, gr	10YR 2/1	S, FR, po, so, NC	-	-	3, vf/f	3, f/m
AEn	10-37	C-S	1, m, abk	10YR 3/3	S, FR, po, so, NC	-	-	2, vf/f/m	2, f
En	37-52	C-S	2, f, abk	10YR 2/1	S, FR, po, so, NC	-	-	2, vf/f/m	
Env	52-70	C-S	2, f/m, abk	10YR 4/3	S, FR, po, so, NC	F3M,f, 2, F, D, I, C	10YR 5/8	2, vf/f/m	3, f/m
EB	70-95	C-S	2, m/vc, abk	10YR 4/3	S, FR, po, so, NC	F3M,f, 2, F, D, I, C	10YR 5/3	2, f/m	3, f/m
Btn	95-125+		2, m/vc, abk	10YR 3/1	SH, FR, po, so, NC	-	-	1, vf/f	2, f/m
S9 - Eutric Leptosol (Loamic, Ochric, Yermic)/ NEOSSOLO LITÓLICO Eutrófico típico									
A	0-20	A-S	2, m, sbk	10YR 4/2	FR, po, so, NC	-	-	3, vf/f/m	2, f/m
R	20+	-	-	-	-	-	-	-	-
Highlands in plateau									
S4 - Xanthic Acrisol (Clayic, Hyperdystric, Ochric, Raptic)/ ARGISSOLO AMARELO Distrófico típico									
A	0-10	G-S	1, f/m, sbk	10 YR 4/3	S, FR, po, so, NC	-	-	3, vf/f/m	3, f/m
2Ab	10-50	D-S	2, f/m, sbk	10 YR 6/4	SH, FR, po, so, NC	-	-	2, vf/f/m	3, f/m/co
2Bto	50-120+		2, f/m, sbk	10 YR 7/4	SH, FR, ps, ss, NC	-	-	2, vf/f	3, f/m
S6 - Hypereutric Arenosol (Ochric)/ NEOSSOLO QUARTZARÊNICO Órtico léptico									
A1	0-3	C-S	2, f/m,sbk	2.5Y 4/3	FR, po, so, NC	-	-	1, vf	1, vf
A2	3-8	G-S	2, m/co, sbk	2.5Y 4/4	FR, po, so, NC	-	-	1, vf	1, vf
A3	8-13	G-S	2, m/co, sbk	2.5Y 3/3	FR, po, so, NC	-	-	3, vf	3, vf/f/m

AC	13-28	C-S	2, f, sbk	2.5Y 3/3	S, FR, po, so, NC	-	-	2, vf/f/m	2, f/m
C	28-70	C-S	2, m, sbk	2.5Y 4/4	S, FR, po, so, NC	-	-	2, vf/f	3, f/m
R	70+								
S10 – Geric Pisoplinthic Plinthosol (Clayic, Eutric, Ochric, Raptic)/ PLINTOSSOLO PÉTRICO Concrecionário êutrico									
Ac	0-3	C-W	2, m, sbk	2.5YR 3/2	FR, ps, s, NC	FSN, m, 2, P, D, I, S	10R 4/6	1, f	2, f/m
Bc1	3-30	C-S	2, m,sbk	2.5YR 4/3	FR, p, ss, NC	FSN, m, 3, P, D, I, S	10R 4/6	2, vf/f	2, f/m
Bc2	30-50	C-S	2, f, sbk	2.5YR 4/6	FR, p, s, NC	FSN, m, 4, P, D, I, S	10R 4/6	1, vf	2, vf/f
Bm	50+	-	-	-	-	-	-	-	-

Distinctness: A=abrupt, C=clear, D=diffuse; G=gradual. Topography: S=smooth, W=wavy. Structure: Grade: 1=weak, 2=moderate. Size: co=coarse, f=fine, m=medium, vc=very coarse. Type: abk=angular block, cpr=columnar, gr=granular, m=massive, pr=prismatic, sbk= subangular block. /=principal structure parting to secondary one. Consistence: Dry: EH=extreme hard, EF=extreme firm, HA=hard, L= loose, S=soft, SH=slightly hard. Moist: FR= friable, L=loose. Wetter: so=nonsticky, ss= slightly sticky, p=moderately plastic, po=nonplastic, ps= slightly plastic. Cementation: M=moderately cemented, NC= non-cemented. Redoximorphic features: Kind: F3M=noncemented Fe^{3+} mass, FSN=ironstone. Quantity: f=few, m=many. Size: 2=medium, 3=coarse, 4=very coarse. Contrast: F=faint, P=prominent. State: D=dry. Hardness: I=indurated. Boundary: C=clear, S=sharp. Roots and pores: 1= few, 2= common, 3=many, co=coarse, f=fine, m= medium, vf=very fine.

Coarse sand is the dominant particle in most profiles (Table 3). The texture varies between clay and loamy sand. Overall, clay content increases in depth. Soils range from extremely acidic to strongly alkaline (Table 4). The coarse sand/fine sand and/or sand/silt ratios indicated lithic discontinuity in all soil profiles, except for one Arenosol, one Leptosol and one Regosol. The pH H_2O values are higher than pH KCl. The Plintosol register ΔpH close to zero. Ca^{2+}>Mg^{2+}>K^{+}>Na^{+} is the dominance of bases in all horizons, except among the Solonetz. The Al^{3+} contents were below 1 cmolc kg^{-1} in all horizons. All profiles have base saturation greater than 50%, except Acrisol. The coarse sand/fine sand ratio indicates lithic discontinuity at 10 cm of depth in Acrisol.

Table 3. Physical soil properties

Horizon	Depth (cm)	Coarse sand	Fine sand	Silt	Clay	Coarse sand / Fine sand	Sand / Silte	Silt/Clay	Texture
			%						
Lowlands in pediment plain									
S1 – Eutric Leptosol (Loamic, Humic, Yermic, Raptic)/ NEOSSOLO LITÓLICO Eutrófico fragmentário									
A	0-7	36	35	18	11	1.0	3.9	1.61	sandy loam
Cr	0-25	53	9	22	16	5.8	2.8	1.44	sandy loam
R	25+	-	-	-	-	-	-	-	-
S2 –Leptic Abruptic Luvisol (Clayic, Cutanic, Differentic, Hypereutric, Ochric, Raptic)/ LUVISSOLO CRÔMICO Órtico típico									
A	0-30	40	27	18	15	1.5	3.7	1.14	sandy loam
Bt	30-47	22	11	18	49	2.0	1.8	0.36	clay
Cr	47-70	33	18	18	31	1.8	2.8	0.58	sandy clay loam
R	70+	-	-	-	-	-	-	-	-
S3 - Hypereutric Regosol (Loamic, Ochric, Yermic, Raptic)/ NEOSSOLO REGOLÍTICO Eutrófico típico									
A	0-65	20	23	25	33	0.9	1.7	0.76	clay loam
Cr	65-112	41	22	29	9	1.9	2.1	3.33	sandy loam
R	112+	-	-	-	-	-	-	-	-
S5 - Stagnic Abruptic Solonetz (Clayic, Columnic, Cutanic, Differentic, Ochric, Magnesic, Hypernatric, Raptic)/ PLANOSSOLO NÁTRICO Órtico dúrico									
An_1	0-10	34	41	13	12	0.8	5.8	1.11	sandy loam
An_2	10-37	33	51	7	9	0.6	12.0	0.86	loamy sand
$Btnv_1$	37-48	35	31	8	26	1.1	8.3	0.3	sandy clay loam
$Btnv_2$	48-115+	15	12	11	62	1.3	2.5	0.18	clay
S7 - Hypereutric Regosol (Loamic, Ochric, Yermic)/ NEOSSOLO LITÓLICO Eutrófico típico									
A	0-19	41	26	17	16	1.6	3.9	1.01	sandy loam
AC	19-45	40	21	18	21	1.9	3.4	0.84	sandy clay loam
R	45+	-	-	-	-	-	-	-	-

S8 - Stagnic Solonetz (Albic, Loamic, Ochric, Magnesic, Hypernatric, Raptic)/ PLANOSSOLO NÁTRICO Órtico típico									
A	0-10	10	58	20	13	0.2	3.4	1.59	sandy loam
AEn	10-37	22	59	11	8	0.4	7.4	1.33	loamy sand
En	37-52	22	53	15	10	0.4	5.0	1.44	sandy loam
Env	52-70	24	62	7	7	0.4	12.3	0.93	loamy sand
EB	70-95	14	62	14	11	0.2	5.4	1.27	sandy loam
Btn	95-125+	9	43	24	25	0.2	2.2	0.96	sandy clay loam
S9 - Eutric Leptosol (Loamic, Ochric, Yermic)/ NEOSSOLO LITÓLICO Eutrófico típico									
A	0-20	40	39	9	12	-	-	0.71	sandy loam
R	20+	-	-	-	-	-	-	-	-
Highlands in plateau									
S4 - Xanthic Acrisol (Clayic, Hyperdystric, Ochric, Raptic)/ ARGISSOLO AMARELO Distrófico típico									
A	0-10	16	15	10	59	1.1	3.1	0.18	clay
2Ab	10-50	62	19	3	16	3.3	27.0	0.21	sandy loam
2Bt	50-120+	17	16	11	56	1.1	3.0	0.19	clay
S6 - Hypereutric Arenosol (Ochric)/ NEOSSOLO QUARTZARÊNICO Órtico léptico									
A_1	0-3	69	13	8	10	5.3	10.3	0.84	loamy sand
A_2	3-8	72	12	10	6	6.0	8.4	1.61	loamy sand
A_3	8-13	74	11	10	6	6.7	8.5	1.69	loamy sand
AC	13-28	74	11	8	7	6.7	10.6	1.16	loamy sand
C	28-70	72	12	9	7	6.0	9.3	1.19	loamy sand
R	70+	-	-	-	-	-	-	-	-
S10 - Geric Plinthosol (Clayic, Eutric, Ochric, Raptic)/ PLINTOSSOLO HÁPLICO Eutrófico petroplíntico									
Ac	0-3	22	8	12	58	2.8	2.5	0.21	clay
Bc_1	3-30	22	7	13	59	3.1	2.2	0.21	clay
Bc_2	30-50	14	8	13	65	1.8	1.7	0.2	clay
Bm	50+	-	-	-	-	-	-	-	-

Table 4. Chemical soil properties

Horizon	Depth cm	pH H_2O	pH KCl	P_M mg kg^{-1}	K^+	Na^+	Ca^{2+}	Mg^{2+}	Al^{3+}	H+Al	ECEC	CEC	ISNa	V	COS	N	C/N	P_{REM} mgL^{-1}
					---------------------------------- cmolc kg^{-1} -------------------------------								--------------- % ------------					
Lowlands in pediment plain																		
S1 – Eutric Leptosol (Loamic, Humic, Yermic, Raptic)/ NEOSSOLO LITÓLICO Eutrófico fragmentário																		
A	0-7	4.8	3.6	9	<1	<1	2.2	0.7	0.6	4.7	3.9	8.0	1	41	1.95	0.11	18	45.3
Cr	7-25	5.1	3.4	2	<1	<1	2.0	1.3	1.0	1.9	4.5	5.4	2	65	0.45	0.04	12	46.7
R	25+	-	-	-	-	-	-	-	-	-	-	-	-	-	-	-	-	-
S2 –Leptic Abruptic Luvisol (Clayic, Cutanic, Differentic, Hypereutric, Ochric, Raptic)/ LUVISSOLO CRÔMICO Órtico típico																		
A	0-30	6.0	5.0	8	<1	<1	5.3	1.5	<0.1	1.6	7.4	9.0	1	82	1.20	0.10	12	48.6
Bt	30-47	6.0	3.5	2	<1	<1	16.2	7.5	0.3	2.6	24.4	26.7	1	90	0.45	0.05	87	35.4
Cr	47-70	6.2	3.8	2	<1	<1	14.6	9.1	0.2	1.4	24.3	25.5	2	95	0.30	0.03	10	43.6
R	70+	-	-	-	-	-	-	-	-	-	-	-	-	-	-	-	-	-
S3 - Hypereutric Regosol (Loamic, Ochric, Yermic, Raptic)/ NEOSSOLO REGOLÍTICO Eutrófico típico																		
A	0-65	6.4	4.9	65	1	<1	18.5	11.5	<0.1	1.0	30.6	31.6	1	97	0.82	0.06	14	43.2
Cr	65-112	7.9	6.0	112	<1	1	28.5	10.4	<0.1	<0.1	39.5	39.5	1	100	0.56	0.01	94	50.0
R	112+	-	-	-	-	-	-	-	-	-	-	-	-	-	-	-	-	-
S5 - Stagnic Abruptic Solonetz (Clayic, Columnic, Cutanic, Differentic, Ochric, Magnesic, Hypernatric, Raptic)/ PLANOSSOLO NÁTRICO Órtico dúrico																		
An_1	0-10	5.4	5.1	14	<1	1	4.1	2.2	<0.1	1.4	7.7	9.1	14	85	1.42	0.11	13	53.9
An_2	10-12	5.3	4.8	5	<1	1	2.8	1.4	<0.1	0.6	5.3	5.9	15	90	0.38	0.03	12	54.5
Btn_1	12-48	5.6	5.2	2	<1	7	6.7	6.5	<0.1	0.3	20.3	20.6	34	99	0.38	0.04	92	46.2
Btn_2	48-115+	7.4	5.9	2	<1	5	2.3	2.6	<0.1	0.0	9.7	9.7	49	100	0.23	0.02	12	49.2
S7 - Hypereutric Regosol (Loamic, Ochric, Yermic)/ NEOSSOLO LITÓLICO Eutrófico típico																		
A	0-19	5.6	4.4	50	<1	<1	3.6	3.0	<0.1	1.1	6.9	8.0	3	86	0.39	0.05	7	54.0
AC	19-45	6.6	4.3	68	<1	2	5.4	7.9	<0.1	0.6	15.9	16.5	15	96	0.08	0.04	2	51.3
R	45+	-	-	-	-	-	-	-	-	-	-	-	-	-	-	-	-	-

S8 - Stagnic Solonetz (Albic, Loamic, Ochric, Magnesic, Hypernatric, Raptic)/ PLANOSSOLO NÁTRICO Órtico típico																		
A	0-10	6.6	6.0	99	1	<1	4.9	1.4	<0.1	0.2	7.1	7.3	1	97	1.56	0.14	11	56.0
AEn	10-37	6.4	5.8	92	<1	1	3.3	1.3	<0.1	<0.1	5.9	5.9	14	100	0.23	0.04	6	55.5
En	37-52	6.9	6.1	51	1	4	4.3	1.3	<0.1	<0.1	10.1	10.1	38	100	0.31	0.03	9	53.7
Env	52-70	7.4	6.4	104	<1	3	1.5	1.4	<0.1	<0.1	6.2	6.2	48	100	0.08	0.02	4	56.6
EB	70-95	8.7	7.5	21	<1	4	1.6	1.7	<0.1	<0.1	7.7	7.7	52	100	0.08	0.02	4	57.0
Btn	95-125+	8.6	7.1	13	<1	9	1.7	2.1	<0.1	<0.1	13.4	13.4	68	100	0.20	0.04	5	47.8
S9 - Eutric Leptosol (Loamic, Ochric, Yermic)/ NEOSSOLO LITÓLICO Eutrófico típico																		
A	0-20	4.4	3.7	3	<1	<1	1.2	0.2	0.3	1.3	2.1	3.0	<1	58	0.47	0.05	10	55.0
R	20+	-	-	-	-	-	-	-	-	-	-	-	-	-	-	-	-	-
Highlands in plateau																		
S4 - Xanthic Acrisol (Clayic, Hyperdystric, Ochric, Raptic)/ ARGISSOLO AMARELO Distrófico típico																		
A	0-10	4.9	3.7	6	<1	<1	0.6	0.2	0.3	1.6	1.1	2.4	<1	34	0.52	0.03	21	54.5
2Ab	10-50	4.6	3.7	2	<1	<1	0.2	0.1	0.6	1.4	0.9	1.7	<1	19	0.30	0.02	14	53.5
2Bt	50-120+	4.3	3.8	1	<1	<1	0.2	<0.1	0.9	1.8	1.1	2.1	1	13	0.30	0.02	14	46.1
S6 - Hypereutric Arenosol (Ochric)/ NEOSSOLO QUARTZARÊNICO Órtico léptico																		
A$_1$	0-3	5.5	5.0	4	<1	<1	2.1	0.5	<0.1	0.3	2.7	3.0	<1	90	0.47	0.08	58	58.8
A$_2$	3-8	5.6	4.6	1	<1	<1	1.4	0.2	<0.1	0.5	1.7	2.2	<1	77	0.16	0.02	8	56.9
A$_3$	8-13	5.5	4.4	1	<1	<1	1.1	0.2	<0.1	0.6	1.4	2.0	<1	70	0.16	0.13	1	59.1
AC	13-28	5.5	4.3	1	<1	<1	0.9	0.2	<0.1	0.3	1.2	1.5	<1	79	0.16	0.02	10	57.0
C	28-70	5.5	4.3	0	<1	<1	0.9	0.2	<0.1	0.2	1.1	1.3	<1	85	0.08	0.01	7	59.8
R	70+	-	-	-	-	-	-	-	-	-	-	-	-	-	-	-	-	-
S10 - Geric Plinthosol (Clayic, Eutric, Ochric, Raptic)/ PLINTOSSOLO HÁPLICO Eutrófico petroplíntico																		
Av	0-3	5.1	4.7	4	<1	1	3.5	1.4	<0.1	2.2	6.1	8.3	8	73	1.17	0.10	12	51.8
Bv$_1$	3-30	3.9	3.8	2	<1	2	1.7	1.2	0.6	3.0	6.3	8.7	27	66	0.62	0.06	11	41.8
Bv$_2$	30-50	3.6	3.7	1	<1	3	2.2	1.4	0.9	2.7	8.3	10.2	34	74	0.39	0.04	10	40.8
Bm	50+	-	-	-	-	-	-	-	-	-	-	-	-	-	-	-	-	-

The contents of SOC, N, and P_M decrease with increasing depth, indicating the influence of organic residues on the content of these nutrients. The SOC content in the surface horizon varied between 0.38 and 1.95%. Between 10 and 50 cm depth, the SOC contents varied between 0.08 and 0.42%. The C/N ratio varies between 1 and 93. The P_{REM} contents varied between 35.4 and 59.8 mg L^{-1}. P_{REM} has an inverse relationship with the affinity of P with organic and mineral compounds. The highest values were observed in Arenosol. In turn, the lowest P_{REM} values were recorded by the plinthic horizon of the Plinthosol.

Particle density values is close to quartz and feldspar (Table 5). In general, the bulk density is similar between the horizons of each profile. Bulk density at the surface horizon varies between 0.85 and 1.54 g cm^{-3}. Between 10 and 50 cm the bulk density varied between 0.94 and 1.71 g cm^{-3}. The total porosity ranged from 0.37 m^3 m^{-3} at the argic horizon, of the Acrisol, to 0.67 m^3 m^{-3} at the Solonetz eluvial horizon. The highest values of field capacity and permanent wilting point were recorded by Luvisol and Plinthosol. The values of water available at the surface horizon vary between 0.04 m^3 m^{-3} at Arenosol and 0.12 m^3 m^{-3} at Plinthosol. Between 10 and 50 cm of depth, the values of available water varied between 0.05 m^3 m^{-3}, in Arenosol, and 0.11 m^3 m^{-3}, in Luvisol.

Table 5. Physical soil properties determined in undisturbed samples

Horizon	Depth cm	Particle density	Soil density	Total porosity m³ m⁻³	Field capacity	Wilting point	Available water
		--------- g cm⁻³ -----------			---------------------- kg kg⁻¹ -------------------		
Lowlands in pediment plain							
S1 – Eutric Leptosol (Loamic, Humic, Yermic, Raptic)/ NEOSSOLO LITÓLICO Eutrófico fragmentário							
A	0-7	2.7	1.25	0.54	0.138	0.035	0.103
S2 –Leptic Abruptic Luvisol (Clayic, Cutanic, Differentic, Hypereutric, Ochric, Raptic)/ LUVISSOLO CRÔMICO Órtico típico							
A	0-30	2.69	1.18	0.56	0.167	0.054	0.113
Bt	30-47	2.68	1.14	0.57	0.222	0.111	0.111
S3 - Hypereutric Regosol (Loamic, Ochric, Yermic, Raptic)/ NEOSSOLO REGOLÍTICO Eutrófico típico							
A	0-65	2.89	1.3	0.55	0.233	0.125	0.108
S5 - Stagnic Abruptic Solonetz (Clayic, Columnic, Cutanic, Differentic, Ochric, Magnesic, Hypernatric, Raptic)/ PLANOSSOLO NÁTRICO Órtico dúrico							
Btn1	12-48	2.82	1.43	0.49	0.113	0.039	0.074
S7 - Hypereutric Regosol (Loamic, Ochric, Yermic)/ NEOSSOLO LITÓLICO Eutrófico típico							
A	0-19	2.67	1.37	0.487	0.109	0.039	0.070
AC	19-45	2.67	1.35	0.494	0.137	0.051	0.086
S8 - Stagnic Solonetz (Albic, Loamic, Ochric, Magnesic, Hypernatric, Raptic)/ PLANOSSOLO NÁTRICO Órtico típico							
AEn	10-37	2.56	0.85	0.67	0.151	0.073	0.078
En	37-52	2.6	0.97	0.627	0.181	0.098	0.083
S9 - Eutric Leptosol (Loamic, Ochric, Yermic)/ NEOSSOLO LITÓLICO Eutrófico típico							
A	0-20	2.67	1.11	0.584	0.124	0.042	0.082
Highlands in plateau							
S4 - Xanthic Acrisol (Clayic, Hyperdystric, Ochric, Raptic)/ ARGISSOLO AMARELO Distrófico típico							
A	0-10	2.67	1.54	0.42	0.129	0.030	0.099
2Ab	10-50	2.74	1.71	0.38	0.117	0.032	0.085

2Bt	50-120	2.78	1.74	0.37	0.124	0.045	0.079
S6 - Hypereutric Arenosol (Ochric)/ NEOSSOLO QUARTZARÊNICO Órtico léptico							
A1	0-3	2.74	1.33	0.51	0.075	0.029	0.046
AC	13-28	2.7	1.35	0.5	0.080	0.022	0.058
S10 - Geric Plinthosol (Clayic, Eutric, Ochric, Raptic)/ PLINTOSSOLO HÁPLICO Eutrófico petroplíntico							
Av	0-3	2.56	0.92	0.64	0.259	0.136	0.123

The diagnostic horizons of Luvisol and Planosol show angular blocky and prismatic structures forming an enaulic c/f related distribution pattern with coarse grains and planar voids (Table 6). Fine to very coarse sand blocky angular grains compose the coarse fraction. Fine fraction coats coarse grains. The surface horizon of Arenosol, Leptosols and Regosols shows apedal material forming a chitonic or porphyric c/f related distribution pattern with coarse grains and vugh voids. Smooth fine to very coarse sand blocky angular grains compose the coarse fraction. The diagnostic horizons of Plinthosol and Acrisol show subangular blocky structure forming an enaulic c/f related distribution pattern with coarse grains, channels, and complex packing voids. Smooth silt to coarse sand blocky rounded grains composes the coarse fraction. The fine fraction is opaque and composes peds (Figure 2).

The variation coefficient of aggregate content retained between the 2.00- and 0.25-mm sieves is greater than 20% in all horizons (Table 7). The aggregate content generally has a positive asymmetry, indicating retention of peds retained in the wider sieves. The water stable aggregates content (WSA) varied between 3 and 60%, regardless of the equivalent diameter of the aggregates (Table 7). The lowest levels of WSA were recorded by Arenosol and A and E horizons of Solonetz. The highest levels were recorded by Plinthosol, argic horizon from Solonetz and Luvisol. The WSA has a significant correlation with clay content, CEC, Al^{3+}, H+Al, P_{REM}, SAVI, and altitude (Figure 3).

Table 6. Micromorphological properties of the groundmass of the studied horizons.

Horizon	Depth	Microstructure	Void	C/F ratio and related distribution (limit 2 μm)	Coarse fraction	Fine fraction
Lowlands in pediment plain						
S1 – Eutric Leptosol (Loamic, Humic, Yermic, Raptic)/ NEOSSOLO LITÓLICO Eutrófico fragmentário						
A	0-7	Apedal	Vugh	porphyric	smooth fine to very coarse sand blocky and tabular angular quartz and feldspar grains randomly distributed and poorly sorted.	speckled clay-size 7.5YR 5/6
S2 –Leptic Abruptic Luvisol (Clayic, Cutanic, Differentic, Hypereutric, Ochric, Raptic)/ LUVISSOLO CRÔMICO Órtico típico						
Bt	30-47	Angular blocky	Planar	porphyric	smooth fine to very coarse sand blocky and tabular angular quartz and feldspar grains randomly distributed and poorly sorted.	speckled clay-size 2.5YR 5/6
S3 - Hypereutric Regosol (Loamic, Ochric, Yermic, Raptic)/ NEOSSOLO REGOLÍTICO Eutrófico típico						
A	0-65	Apedal	Vugh	porphyric	smooth fine to very coarse sand blocky and tabular angular quartz and feldspar grains randomly distributed and poorly sorted.	speckled clay-size 7.5YR 5/6
S5 - Stagnic Abruptic Solonetz (Clayic, Columnic, Cutanic, Differentic, Ochric, Magnesic, Hypernatric, Raptic)/ PLANOSSOLO NÁTRICO Órtico dúrico						
Btn_1	12-48	Angular blocky	Planar	enaulic	smooth fine to very coarse sand blocky and tabular angular quartz and feldspar grains randomly distributed and poorly sorted.	speckled clay-size 10YR 5/4
S7 - Hypereutric Regosol (Loamic, Ochric, Yermic)/ NEOSSOLO LITÓLICO Eutrófico típico						
A	0-19	Apedal	Vugh	porphyric	smooth fine to very coarse sand blocky and tabular angular quartz and feldspar grains randomly distributed and poorly sorted.	speckled clay-size 7.5YR 5/6

S8 - Stagnic Solonetz (Albic, Loamic, Ochric, Magnesic, Hypernatric, Raptic)/ PLANOSSOLO NÁTRICO Órtico típico						
Btn	95-125+	Prismatic	Planar	enaulic	smooth fine to very coarse sand blocky and tabular angular quartz and feldspar grains randomly distributed and poorly sorted.	speckled clay-size 10YR 5/4
S9 - Eutric Leptosol (Loamic, Ochric, Yermic)/ NEOSSOLO LITÓLICO Eutrófico típico						
A	0-20	Apedal	Vugh	porphyric	smooth fine to very coarse sand blocky and tabular angular quartz and feldspar grains randomly distributed and poorly sorted.	speckled clay-size 2.5YR 5/6
Highlands in plateau						
S4 - Xanthic Acrisol (Clayic, Hyperdystric, Ochric, Raptic)/ ARGISSOLO AMARELO Distrófico típico						
Bt	50-120+	Subangular blocky	Channel, complex packing	1/1 single-spaced fine enaulic	smooth silt to coarse sand blocky subangular quartz grains randomly distributed and poorly sorted.	undifferentiated clay-size 7.5YR 5/6
S6 - Hypereutric Arenosol (Ochric)/ NEOSSOLO QUARTZARÊNICO Órtico léptico						
A_1	0-3	Apedal	Vugh	chitonic	smooth fine to very coarse sand blocky and tabular angular quartz and feldspar grains randomly distributed and poorly sorted.	undifferentiated clay-size 7.5YR 5/6
S10 - Geric Plinthosol (Clayic, Eutric, Ochric, Raptic)/ PLINTOSSOLO HÁPLICO Eutrófico petroplíntico						
Bv_2	30-50	Subangular blocky	Channel, complex packing	1/1 single-spaced fine enaulic	smooth silt to coarse sand blocky subangular quartz grains randomly distributed and poorly sorted.	undifferentiated clay-size 2.5YR 5/6

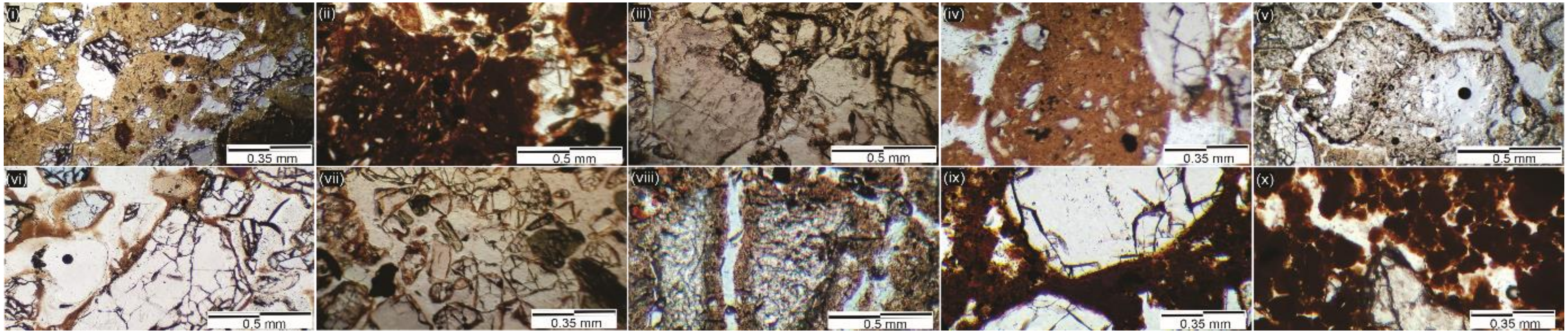

Figure 2. Microphotographies of diagnostic horizons of studied soils: (i) S1 - Eutric Leptosol (Loamic, Humic, Yermic); (ii) S2 - Leptic Abruptic Luvisol (Clayic, Cutanic, Differentic, Hypereutric, Ochric); (iii) S3 - Hypereutric Regosol (Loamic, Ochric, Yermic); (iv) S4 - Xanthic Acrisol (Clayic, Hyperdystric, Ochric, Raptic); (v) S5 –Stagnic Abruptic Solonetz (Clayic, Columnic, Cutanic, Differentic, Ochric, Magnesic, Hypernatric);(vi) S6 - Hypereutric Arenosol (Ochric); (vii) S7 - Hypereutric Regosol (Loamic, Ochric, Yermic); (viii) S8 - Stagnic Solonetz (Albic, Loamic, Ochric, Magnesic, Hypernatric); (ix) S9 - Eutric Leptosol (Loamic, Ochric, Yermic); (x) S10 - Geric Plinthosol (Clayic, Eutric, Ochric).

Table 7. Water stable aggregates according to size and soil horizon.

Horizon	WSA (%)				MWD
	2 a 4	1 a 2	0.5 a 1	0.25 a 0.5	
			mm		
Lowlands in pediment plain					
S1 – Eutric Leptosol (Loamic, Humic, Yermic, Raptic)/ NEOSSOLO LITÓLICO Eutrófico fragmentário					
A	12.4^{a}	16.8^{ab}	15.5^{a}	10.0^{a}	1.38
S2 –Leptic Abruptic Luvisol (Clayic, Cutanic, Differentic, Hypereutric, Ochric, Raptic)/ LUVISSOLO CRÔMICO Órtico típico					
A	20.4^{b}	23.8^{b}	18.3^{ab}	14.3^{b}	1.46
Bt	16.6^{ab}	54.6^{c}	49.2^{c}	53.5^{c}	1.01
S3 - Hypereutric Regosol (Loamic, Ochric, Yermic, Raptic)/ NEOSSOLO REGOLÍTICO Eutrófico típico					
A	30.7^{c}	51.7^{c}	42.3^{d}	36.9^{d}	1.27
S5 - Stagnic Abruptic Solonetz (Clayic, Columnic, Cutanic, Differentic, Ochric, Magnesic, Hypernatric, Raptic)/ PLANOSSOLO NÁTRICO Órtico dúrico					
An_1	5.4^{d}	11.6^{d}	14.8^{ab}	10.9^{a}	1.08
An_2	4.1^{d}	8.6^{de}	10.0^{e}	9.8^{a}	1.04
Btn_1	7.2^{d}	5.9^{e}	3.3^{g}	3.0^{f}	1.72
S7 - Hypereutric Regosol (Loamic, Ochric, Yermic)/ NEOSSOLO LITÓLICO Eutrófico típico					
A	10.4^{a}	7.5^{e}	8.1^{e}	10.1^{a}	1.38
AC	22.3^{b}	20.4^{b}	16.5^{ab}	32.3^{d}	1.24
S8 - Stagnic Solonetz (Albic, Loamic, Ochric, Magnesic, Hypernatric, Raptic)/ PLANOSSOLO NÁTRICO Órtico típico					
A	31.8^{c}	30.0^{f}	29.5^{g}	21.5^{e}	1.47
AEn	30.4^{c}	26.4^{b}	23.1^{f}	17.3^{b}	1.55
En	46.1^{e}	18.3^{b}	17.5^{ab}	10.1^{a}	1.96
Env	29.5^{c}	15.0^{a}	14.9^{ab}	6.1^{g}	1.87
EB	8.8^{d}	20.5^{b}	12.3^{e}	8.3^{a}	1.35
Btn	13.5^{a}	24.4^{b}	17.9^{ab}	6.9^{g}	1.46
S9 - Eutric Leptosol (Loamic, Ochric, Yermic)/ NEOSSOLO LITÓLICO Eutrófico típico					
A	14.9^{a}	15.3^{a}	11.4^{e}	6.2^{g}	1.61
Highlands in plateau					
S4 - Xanthic Acrisol (Clayic, Hyperdystric, Ochric, Raptic)/ ARGISSOLO AMARELO Distrófico típico					
A	16.2^{ab}	11.3^{d}	12.8^{e}	15.5^{b}	1.38
2Ab	19.3^{b}	15.7^{a}	19.7^{b}	22.2^{e}	1.28
2Bt	16.2^{ab}	15.2^{a}	22.6^{f}	27.7^{d}	1.12
S6 - Hypereutric Arenosol (Ochric)/ NEOSSOLO QUARTZARÊNICO Órtico léptico					
A_1	6.6^{d}	14.0^{a}	19.3^{b}	5.9^{g}	1.22
A_3	2.5^{d}	3.4^{e}	3.3^{g}	3.9^{f}	1.19
S10 - Geric Plinthosol (Clayic, Eutric, Ochric, Raptic)/ PLINTOSSOLO HÁPLICO Eutrófico petroplíntico					
Av	62.7^{e}	64.0^{c}	38.6^{d}	53.4^{c}	1.46

Bv_1	28.2^{b}	47.9^{g}	51.3^{h}	62.0^{h}	1.07
Bv_2	45.0^{e}	46.4^{g}	50.3^{h}	62.5^{h}	1.22
Previous studies					
0-10 cm layer[α]					0.99
10-20 cm layer[α]					0.81
20-30 cm layer[α]					1.07
0-10 cm layer[β]					2.09
10-20 cm layer[β]					1.73
20-30 cm layer[β]					1.99
Shrub/0-5 cm layer[γ]					1.13
Shrub/5-20 cm layer[γ]					1.54
Shrub/20-40 cm layer[γ]					0.82
Shrub/40-60 cm layer[γ]					0.35
Shrub/60-100 cm layer[γ]					0.27
Grassland/0-10 cm layer[δ]					1.75
Grassland/0-10 cm layer[δ]					2.13
Grassland/0-10 cm layer[δ]					1.42
Grassland/0-10 cm layer[δ]					1.60

* Different lowercase letters indicate significant differences among the study sites for the same aggregate size using Tukey's HSD test ($p < 0.05$). [α]=Silva et al., 2021. [β]=Medeiros et al., 2023. [γ] = Liu et al., 2014. [δ] = Liu et al., 2021.

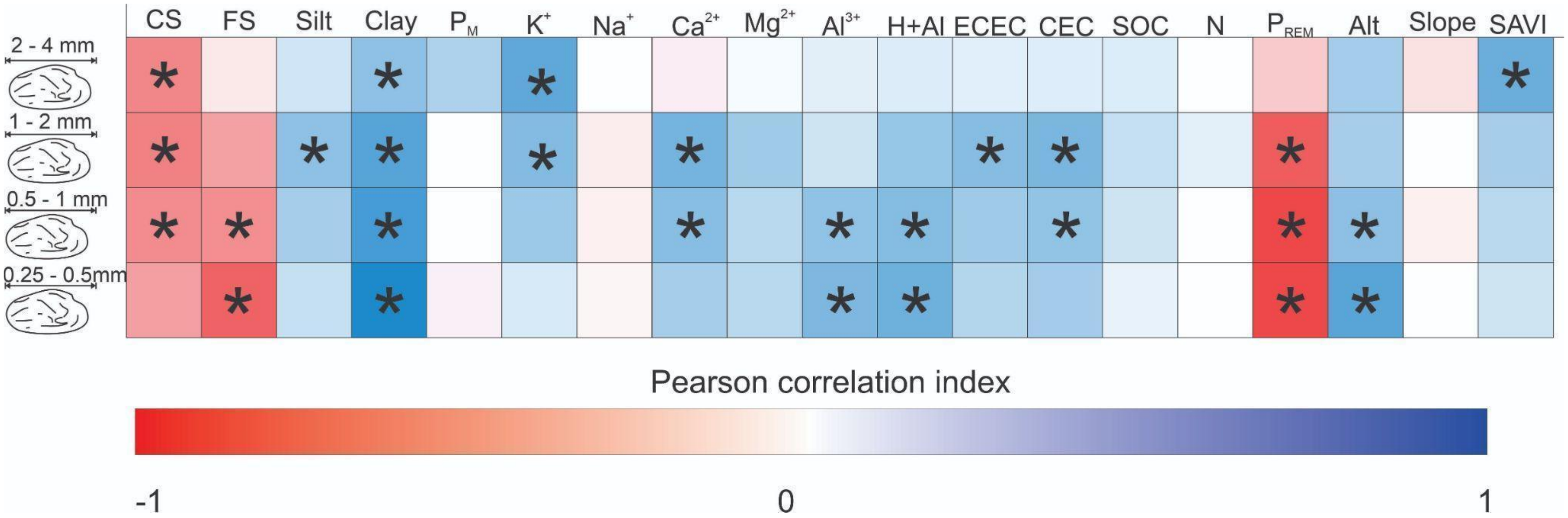

Figure 3. Correlation matrix between WSA and soil properties according to aggregate diameter. CS= coarse sand, FS= fine sand, P_M=Mehlich-1 extractable PECEC=effective cationic exchange capacity, CEC=cationic exchange capacity, SOC=soil organic matter, P_{REM}= P adsorption capacity, Alt=altitude. * = significant correlation at p<0.05 according to t test.

5. Discussion

Pedogenesis acts differently in ped formation and stabilization of aggregates (Table 7). The low variation of mean weighed diameter (MWD) of wet stable aggregates among soil profiles in this study suggests that differences of soil formation processes are not crucial to define ped size. On the other hand, differences between water stable aggregates (WSA) indicates that physical and chemical processes are relevant to ped stability. The high ped stability in Luvisol and Solonetz is attributed to ped formation in these soils. Shrinking-swelling of high-activity clays orient and compress clay, creating aggregated and voids (DIEL et al., 2019; WOLKA et al., 2021). The water infiltration in the wet season favors adhesion among clay particles. The loss of water in the dry season induces flocculation of these particles. The high specific surface of these clays guarantees a strong grade structure. On the other hand, aggregation in soils with low-activity clays evolves biological activity and weathering residues (YIN et al., 2016; TOTSCHE et al., 2018b). Iron and aluminum oxides expose positive charges on surface due to their high PCZ. The positive charges are neutralized by organic matter and kaolinite. Organisms such as termites and worms ingest flocculated particles, which are partially digested. After they have been defecated, these particles are cemented by hyphae and dehydration. In both ped formation ways, the clay content is a crucial parameter.

The WSA of equivalent diameter between 2 and 4 mm varied between 2.5 and 62.7%. The lowest values were recorded by Arenosol and Solonetz surface horizons. The highest values were recorded by the Plinthosol and argic horizon of Solonetz. Correlation analysis suggests different mechanisms responsible for stabilizing aggregates of different sizes. SAVI, clay, and sand contents are important for aggregates larger than 1 mm. The CEC, P_{REM}, Al^{3+}, and altitude are important for aggregates smaller than 1 mm. Texture influences the shape, stability, and resilience of soil aggregates and the response of this structure to climatic and biological factors (WEI et al., 2016; SHI et al., 2017). Clay covers sand grains and fills the interstices of these larger grains, increasing the cohesion between particles and, consequently, the stability of the aggregates (DIECKOW et al., 2009; STOOPS and SCHAEFER, 2010). Similar results were observed in soil in the Brazilian Savanna. The increase of clay content increased aggregate stability due to stronger affinity between clay minerals, Fe-oxides and organic particles (SALTON et al., 2008).

The generalized difference of WSA of equivalent diameter below 2 mm between horizons in the same profile could be attributed to lithic discontinuity and pedogenesis. Differences of parent material, expressed by texture, induces variation of aggregate stability. Weathering of felsic rocks or sedimentary rocks in semiarid regions produces sandy or loamy horizons, while weathering of mafic or metamorphic produces clayey horizons (ARAÚJO FILHO et al., 2023). Besides, differences of parent material also can be extended to mineralogy, although this study did not present XRD data. Texture and mineralogy are directly related to specific surface of particles, CEC and water retention capacity of soil. All these variables will influence pedalization (KAISER and GUGGENBERGER, 2003; GUGGENBERGER and KAISER, 2003; SOLLINS et al., 2009) by bioturbation, microorganisms' activity and flocculation of particles. Termites ingest and partially digest clay minerals because of the high pH in their intestine (SOUZA et al., 2020). The excreta is rich in organic matter, low crystalline minerals and water (FREITAS et al., 2021; SARCINELLI et al., 2009). Polysaccharide (SIX et al., 2004), proteinaceous (KLEBER et al., 2007) and lipid (JANDL et al., 2004; LIU et al., 2013) create organo-metallic complexes crucial to flocculation of particles and ped formation. The encrustation of Al- and Fe-oxides, and clay minerals around organic matter create very stable clay-organic matter microaggregates (SIX and JASTROW, 2002). Living microorganisms also induce microaggregation by adhering to clay particles by direct electrostatic bonds (HUANG et al., 2005). Stability of these peds is kept once even after death, the bacterium cell wall persists (AMELUNG et al., 2008). Absence of correlation between WSA and organic carbon could be attributed to low input of organic residues in semiarid regions (SOUZA et al., 2022).

On the other hand, processes as elutriation and lessivage also contribute to differences of aggregate stability between horizons due to texture variation (BISSONAIS, 1996). Elutriation is a process of texture differentiation between horizons due to erosion of clay in the surface horizon. The low vegetation cover and torrential rains promotes destruction of aggregates by collision between rain drop and soil (splash effect) and microsealing of soil surface (CÂMARA et al., 2021). These effects reduce water infiltration and induce preferential erosion of fine particles, decreasing the content of clay in the surface horizon. Lessivage is a process of clay translocation from topsoil to subsurface horizons. Clay migrates through voids by gravity effect and water percolation (QUÉNARD et al., 2011). Previous studies indicated that synergy between anthropic disturbances and torrential precipitation induces runoff and disaggregation of peds (PINHEIRO JÚNIOR et al., 2022). Consequently, microaggregates are dominant. On the other hand, pristine sites present higher soil organic matter content and aggregate stability of peds larger than 2 mm (MARCOLAN & ANGHINONI, 2006; LIMA et al., 2008; SILVA,2021).

Higher SAVI values indicate a higher density of vegetation cover. Roots exude organic compounds that contribute to aggregate formation. These substances (polysaccharides, alcohols, tannins, etc.) are excreted at the root-soil interface and cement the mineral particles (ZHENG et al., 2016; ERKTAN et al., 2017). Roots are also responsible for material compression during the growth and formation of channels and aggregates (STOLT and LINDBO, 2010). In addition, the rhizosphere hosts a microbial community that excretes extracellular polysaccharides that adhere to soil mineral particles and aid in forming aggregates (BERTIN et al., 2003). Soil organic matter is a key factor to aggregate stability in the Brazilian semiarid soils (MAIA et al.,2006, MEDEIROS et al., 2023).

Physicochemical mechanisms are more relevant in the stability of smaller aggregates. The role of Al^{3+} as flocculating agent is well known due to the compression of the diffuse double layer (TOTSCHE et al., 2018). However, due to low leaching and incipient weathering, the soils in Brazilian semiarid commonly are virtually free of Al^{3+}, except for Acrisols, Plinthosol and Arenosols developed from sandstones (ARAÚJO et al., 2017). So, Al^{3+} plays a limited role in aggregate stability in semiarid soils. On the other hand, the Brazilian semiarid soils have high CEC and high activity clays. These particles are negatively charged and present a high affinity to each other once soils are sticky. The expansion and retraction of soil mass during wetting-drying cycles induce the formation of strong-grade peds (DENEF and SIX, 2005; DIEL et al., 2019; PEREIRA et al., 2021).

The inverse correlation between P_{REM} and aggregate stability indicates the role of positive particles, such as goethite and hematite, in aggregation. Unlike most silicates, iron oxides have a high affinity for P and generate positive charges due to their high point of zero charge (MADRID and ARAMBARRI, 1985). The higher positive charges amount favors charge neutralization and aggregate stability compared to soils with high P_{REM} (WEI *et al.*, 2016). The significant correlation between altitude and aggregate stability could be related to the topographic distribution of soils. Acrisols, which present high aggregate stability, cover the highlands, while Planosols and Regosols in the lowlands present low aggregate stability.

Different MWD values can be attributed to land use (Table 7). Ped destruction by overgrazing is well known (MEDEIROS et al., 2023). Changes in vegetation cover, organic residues input and root depth impact rhizosphere, microbiota composition and decomposition of organic matter (LIU et al., 2014, 2021). Eventual changes in soil chemistry by addition of fertilizer and/or limestone affect positive /negative clay charge balance (CASTRO FILHO et al., 2002).

5.1 Soil fragility and desertification in Brazilian semiarid

Despite its economic and social restructuring, the marks of previous economic cycles were fixed in the form of serious socio-environmental problems in the studied area. The suppression of vegetation for livestock, cotton farming, mining and recent ceramic activities have induced desertification (SANTANA, 2007; CUNHA et al., 2010; IPCC, 2019). This condition can reduce soil capacity to support life, which can lead to rapid fragmentation of native vegetation and reduced water production (ALBALADEJO *et al.*, 1998). Conservation practices that favor coverage and maintenance of soil moisture should be induced by the government and applied by small rural producers to minimize human effects on the environment.

The Brazilian semiarid region is the most populated dry region on the planet and has been experiencing, in recent years, a series of extreme weather events due to climate change. The IPCC report (2019) indicates that approximately 94% of the semiarid region is subject to desertification and that in some regions there is no longer soil biological activity. Future scenarios suggest that the synergy between climate change and anthropization should extend and intensify desertification in the Brazilian semiarid region, reducing biodiversity and food production and inducing rural exodus to large urban centers (IPCC, 2019). In addition, the study points out that the regions with the highest rate of deforestation have been suffering from high temperatures, causing the loss of vegetation and soil biological activity. The report also indicates that these areas until then have had a relatively regulated rainfall regime, which shows that despite the rainfall not having undergone major changes, the loss of soil quality aggravates and causes serious problems. Another aggravating factor is that without vegetation, the soil is more conducive to the action of erosion processes, reducing the chances of recovering the quality of this soil.

6. Conclusions

The soil fragility is fundamental for understanding the erosion processes in the Brazilian semiarid region. Large and fine aggregates presented different stability mechanisms. SAVI, clay, and sand contents are important for aggregates larger than 1 mm. The CEC, P_{REM}, Al^{3+}, and altitude are important for aggregates smaller than 1 mm. Due to lower clay and SOC content, Arenosols and Leptosols are more sensitive to soil loss than Luvisols, Planosols and Plinthosols. The aggregate stability of is also attributed as a response to morphogenesis-pedogenesis dynamic. Low activity clays associated to voids formed by bioturbation induces higher water percolation and leaching in Acrisols. Consequently, the runoff and soil loss are lower than soils as Luvisols and Planosols which present abrupt textural change and voids formed by cracks. The data provided by the research are essential for advancing hydro-erosive studies in a semiarid environment, as they can also support the elaboration of public policies aimed at the planning and management of rural spaces.

Contribuições dos Autores: Concepção, V.L.C.O., J.J.L.L.S.; metodologia, V.L.C.O., J.J.L.L.S.; software, J.N.C.; validação, V.L.C.O., J.N.C.; análise formal, V.L.C.O., J.N.C.; pesquisa, V.L.C.O., J.N.C., L.A.C., J.J.L.L.S.; recursos, V.L.C.O., L.A.C., J.J.L.L.S.; preparação de dados, V.L.C.O., J.N.C., L.A.C., J.J.L.L.S.; escrita do artigo, V.L.C.O., J.N.C., L.A.C., J.J.L.L.S.; revisão, V.L.C.O., J.N.C., L.A.C., J.J.L.L.S.; supervisão, L.A.C., J.J.L.L.S.; aquisição de financiamento, L.A.C., J.J.L.L.S.

Todos os autores leram e concordaram com a versão publicada do manuscrito.

Financiamento: Esta pesquisa não recebeu nenhum financiamento externo.

Agradecimentos: V.L.C.O. e J.N.C. agradecem à CAPES pela conceção da bolsa. J.J.L.L.S. agradece à CAPES pela bolsa produtividade PQ2.

Conflito de Interesse: Os autores declaram não haver conflito de interesse.

References

1. ALBALADEJO J.; MARTINEZ-MENA M.; ROLDAN A.; CASTILLO V. Soil degradation and desertification induced by vegetation removal in a semiarid environment. **Soil Use and Management**. v.14, p. 1-5, 1998. DOI: 10.1111/j.1475-2743.1998.tb00602.x
2. ALVES W. DE. F; MOTA A. S.; LIMA, R. A. A; BELLEZONI R.; VASCONCELLOS A. Termites as Bioindicators of Habitat Quality in the Caatinga, Brazil: Is There Agreement Between Structural Habitat Variables and the Sampled Assemblages? **Neotropical Entomology**. v. 40, p. 39-46, 2011. DOI: 10.1590/S1519-566X2011000100006
3. AMELUNG W.; BRODOWSKI S.; SANDHAGE-HOFMANN A.; BOL R. Combining biomarker with stable isotope analyses for assessing the transformation and turnover of soil organic matter. **Advances in Agronomy**. p. 155–250, 2008. DOI: 10.1016/S0065-2113(08)00606-8
4. AMORIM I. L.; SAMPAIO EVSB; ARAÚJO E. L. Flora e estrutura da vegetação arbustivoarbórea de uma área de caatinga do Seridó, RN, Brasil. **Acta Botanica Brasilica**. 19:615-23, 2005. DOI: https://doi.org/10.1590/S0102-33062005000300023
5. ANGELIM L. A. A.; MEDEIROS V. C.; NESI J. R. **Mapa geológico do Estado do Rio Grande do Norte**. Rio grande do Norte: CPRM/FAPERN, 2006. Escala 1:500.000
6. APG. An update of the Angiosperm Phylogeny Group classification for the orders and families of flowering plants. **Botanical Journal of the Linnean Society**. v 181, p. 1-20, 2016. DOI: 10.1111/boj.12385
7. ARAÚJO J. C. F.; RIBEIRO M. R.; BURGOS N.; MARQUES F.A. Solos da Caatinga. In: Curi N, Ker JC, Novais RF, Vidal-Torrado P, Schaefer CEGR, editors. Pedologia - Solos dos Biomas Brasileiros. Viçosa-MG: **Sociedade Brasileira de Ciência do Solo**; 2017. p. 227-60.
8. ARAÚJO FILHO, J.C.; CORREIA, M. M.; PAIVA, A. Q.; COSTA, O. V.; VALLADARES, G. S.; RIBEIRO, M. R.; SCHAEFER, C. E. G. R. Semi-arid Soils of the Caatinga Biome of Northeastern Brazil. In: Schaefer CEGR, editor. The Soils of Brazil. World Soils Book Series. Cham**: Springer**. p.175-193, 2023. DOI: 10.1007/978-3-031-19949-3_6
9. BAKKER M. M.; GOVERS G.; KOSMAS C.; VANACKER V.; OOST K VAN, ROUNSEVELL M. Soil erosion as a driver of land-use change. **Agriculture, Ecosystems and Environment**. 105:467-81, 2005. DOI: 10.1016/j.agee.2004.07.009
10. BERTIN C., YANG X., WESTON L.A. The role of root exudates and allelochemicals in the rhizosphere. **Plant and Soil**. 256:67-83, 2003.DOI: 10.1023/A:1026290508166
11. BISSONNAIS Y. Aggregate stability and assessment of soil crustability and erodibility: I. Theory and methodology. **European Journal of Soil Science**. n. 47, p. 425–437, 1996. DOI: 10.1111/j.1365-2389.1996.tb01843.x
12. BLAUD A.; CHEVALLIER T.; VIRTO I.; PABLO A. L.; CHENU C.; BRAUMAN A. Bacterial community structure in soil microaggregates and on particulate organic matter fractions located outside or inside soil macroaggregates. **Pedobiologia.** 57:191-4, 2014. DOI: 10.1016/j.pedobi.2014.03.005

13. CÂMARA E.R.G.; SANTOS J.C.B.; ARAÚJO FILHO J.C.; SCHULZE S.M.B.B.; CORRÊA M.M.; FERREIRA T.O.; SOUSA J.E.S.; SOUZA JÚNIOR V.S. Parent rock–pedogenesis relationship: How the weathering of metamorphic rocks influences the genesis of Planosols and Luvisols under a semiarid climate in NE Brazil. **Geoderma**. 385, 2021. DOI: 10.1016/j.geoderma.2020.114878
14. CASTRO FILHO C.; LOURENÇO A.; GUIMARÃES M. F.; FONSECA I. C. B. Aggregrate stability under different soil management systems in a red latosol in the state od Paraná, Brazil. **Soil & Tillage Research**. 65:45-51, 2002.
15. CHARTIER M. P.; ROSTAGNO C. M.; VIDELA L. S. Selective erosion of clay, organic carbon and total nitrogen in grazed semiarid rangelands of northeastern Patagonia, Argentina. **Journal of Arid Environments**. 88:43-9, 2013. DOI: 10.1016/j.jaridenv.2012.08.011
16. CUNHA T. J. F.; PETRETE V. G.; SILVA D. J.; MENDES A. M. A.; MELO R. F. DE OLIVEIRA NETO M. B. DE, SILVA M. S. L. DA, ALVAREZ I. A. Principais solos do Semiárido tropical brasileiro: caracterização, potencialidades, limitações, fertilidade e manejo. **Semiárido Brasileiro: Pesquisa, Desenvolvimento e Inovação**. 402, 2010.
17. DENEF K.; SIX J. Clay mineralogy determines the importance of biological versus abiotic processes for macroaggregate formation and stabilization**. European Journal of Soil Science**. 56:469-79, 2005. DOI: 10.1111/j.1365-2389.2004.00682.x
18. DIECKOW J.; BAYER C.; CONCEIÇÃO P. C.; ZANATTA J. A.; MARTIN-NETO L.; MILORI D. B. M.; SALTON J. C.; MACEDO M. M.; MIELNICZUK J.; HERNANI L. C. Land use, tillage, texture and organic matter stock and composition in tropical and subtropical Brazilian soils. **European Journal of Soil Science.** 60:240-9, 2009. DOI: 10.1111/J.1365-2389.2008.01101.X
19. DIEL J.; VOGEL H. J.; SCHLÜTER S. Impact of wetting and drying cycles on soil structure dynamics. **Geoderma**. 345:63-71, 2019. DOI: 10.1016/j.geoderma.2019.03.018
20. SANTOS L. L. Quantificação do escoamento superficial e erosão do solo em regiões semiáridas. **Revista Brasileira de Geografia Física**. 2:14-25, 2009.
21. EMBRAPA. **Uso agrícola dos solos brasileiros**. Rio de Janeiro: Embrapa Solos; 2002.
22. ERKTAN A.; BALMOT J.; MERINO-MARTÍN L.; MONNIER Y.; PAILLER F.; COQ S.; ABIVEN S.; STOKES A.; LE BISSONNAIS Y. Immediate and long-term effect of tannins on the stabilization of soil aggregates. **Soil Biology and Biochemistry**.;105:197-205, 2017. DOI: 10.1016/j.soilbio.2016.11.017
23. FAO. **Soil erosion: the greatest challenge to sustainable soil management**. 2019a. DOI: 10.1080/00050326.1941.10437468
24. FERREIRA C. R. P. C.; ANTONINO A. C. D.; SAMPAIO E. V. DE S. B.; CORREIA K. G.; LIMA JR DE S.; SOARES W. DE A.; MENEZES R. S. C. Soil CO_2 efflux measurements by alkali absorption and infrared gas analyzer in the Brazilian semiarid region. **Revista Brasileira de Ciência do Solo**. 42:1-10, 2018. DOI: 10.1590/18069657rbcs20160563
25. FIDALGO E. C. C.; BENITES V. M.; MACHADO P. L. O. A.; MADARI B. E.; COELHO M. R.; MOURA I. B.; LIMA C. X. Estoque de carbono nos solos do Brasil. **Boletim de Pesquisa e Desenvolvimento/ Embrapa Solos**. 1:27, 2007
26. FITZPATRICK, E. A. Micromorphology of Soils. Dordrecht**: Springer Netherlands**. 1984. DOI: 10.1007/978-94-009-5544-8
27. FREITAS D.F.; KER J.C.; SILVA FILHO L.A. d.; PEREIRA T.T.C.; de SOUZA O.F.F.; SCHAEFER C.E.G.R. Pedogeomorphology and paleoenvironmental implications of large termite mounds at the Brazilian semiarid landscape. **Geomorphology**, 387, 2021. DOI: 10.1016/j.geomorph.2021.107762
28. GARIGLIO M. A.; SAMPAIO E. V. S. B.; CESTARO L. A.; KAGEYAMA P. Y. Uso sustentável e conservação dos recursos florestais da Caatinga. Brasília: **Serviço Florestal Brasileiro**; 2010.
29. GIONGO V.; CUNHA T. J. F.; MENDES A. S.; GAVA C. A.T. Carbono no sistem solo-planta no semiárido brasileiro. **Revista Brasileira de Geografia Física**. 06:1233-53, 2011. DOI: 10.5935/1984-2295.20140015
30. GUGGENBERGER G.; KAISER K. Dissolved organic matter in soil: challenging the paradigm of sorptive preservation. **Geoderma**. n. 113, p. 293–310, 2003. DOI: 10.1016/S0016-7061(02)00366-X
31. HAYNES R.J. Effect of sample pretreatment on aggregate stability measured by wet sieving or turbidimetry on soils of different cropping histories. **European Journal of Science**. n. 44, p. 261–270, 1993.
32. HUANG, P.-M.; WANG, M.-K.; CHIU, C.-Y. Soil mineral-organic matter-microbe interactions: Impacts on biogeochemical processes and biodiversity in soils. **Pedobiologia**. v .9, p. 609–635, 2005. DOI: https://doi.org/10.1016/j.pedobi.2005.06.006
33. IBGE – INSTITUTO BRASILEIRO DE GEOGRAFIA E ESTATÍSTICA. Censo Brasileiro de 2022. Rio de Janeiro: IBGE, 2023.
34. IPCC. Climate change and land: an IPCC special report on climate change, desertification, land degradation, sustainable land management, food security and greenhouse gas fluxes in terrestrial ecosystems. 2019. DOI: 10.4337/9781784710644
35. IUSS WORKING GROUP WRB. World Reference Base for Soil Resources 2014, update 2015 **International soil classification system for naming soils and creating legends for soil maps**. Rome: FAO; 2015. DOI: 10.1017/S0014479706394902
36. IUSS WORKING GROUP WRB. World reference base for soil resources 2014. **International soil classification system for naming soils and creating legends for soil map**s. 2014. DOI: 10.1017/S0014479706394902
37. JANDL G.; LEINWEBER P.; SCHULTEN H.-R.; EUSTERHUES K. The concentrations of fatty acids in organo-mineral particle-size fractions of a Chernozem. **European Journal of Soil Science**. n. 55, p. 459–470, 2004. DOI: 10.1111/j.1365-2389.2004.00623.x

38. KAYANO M. T.; ANDREOLI R. V. Clima da Região Nordeste do Brasil. In: Cavalcanti IF, Ferreira NJ, Silva MGAJ, Dias MAFS, editors. **Tempo e clima no Brasil**. São Paulo: Oficina de textos. p. 213-34, 2009.
39. KAISER K.; GUGGENBERGER G. Mineral surfaces and soil organic matter. **European Journal of Soil Science**. v. 54, p. 219–236, 2003. DOI: 10.1046/j.1365-2389.2003.00544.x
40. KLEBER M.; SOLLINS P.; SUTTON R. A conceptual model of organo-mineral interactions in soils: self-assembly of organic molecular fragments into zonal structures on mineral surfaces. **Biogeochemistry**. n. 85, p. 9–24, 2007. DOI: 10.1007/s10533-007-9103-5
41. LAL R. Digging deeper: A holistic perspective of factors affecting soil organic carbon sequestration in agroecosystems. **Global Change Biology**. 24:3285-301, 2018. DOI: https://doi.org/10.1111/gcb.14054
42. LAL R. Influence of Soil Erosion on Carbon Dynamics in the World. In: Soil erosion and carbon dynamics. In: ROOSE E., LAL R., FELLER C., BARTHÈS B., STEWART B. A., editors. **Advances in soil Science**. Taylor & Francis. p. 23-36, 2006. DOI: 10.1017/S0014479706254103
43. LEHMANN A.; RILLIG M. C. Understanding mechanisms of soil biota involvement in soil aggregation: A way forward with saprobic fungi**? Soil Biology and Biochemistry**. 88:298-302, 2015. https://doi.org/10.1016/j.soilbio.2015.06.006
44. LEITE P. A. M., DE SOUZA E. S., DOS SANTOS E. S., GOMES R. J., CANTALICE J. R., WILCOX B. P. The influence of forest regrowth on soil hydraulic properties and erosion in a semiarid region of Brazil. **Ecohydrology**.11:1-12, 2018. DOI: 10.1002/eco.1910
45. LIMA, J. S. S.; OLIVEIRA, P. C.; OLIVEIRA, R. B.; XAVIER, A. C. Métodos geoestatísticos no estudo da resistência do solo à penetração em trilha de tráfego de tratores na colheita de madeira. **Revista Árvore**. 32:931-938, 2008.
46. LIU X.; EUSTERHUES K.; THIEME J.; CIOBOTA V.; HÖSCHEN C.; MUELLER C. W.; KU¨ SEL K.; KÖGEL-KNABNER I.; RÖSCH P.; POPP J.; TOTSCHE K. U. STXM and NanoSIMS investigations on EPS fractions before and after adsorption to goethite. **Environmental Science and Technology**. n. 47, p. 3158–3166, 2013. DOI: https:10.1021/es3039505
47. LIU M. Y.; CHANG Q. R.; QI Y. B.; LIU J., CHEN T. Aggregation and soil organic carbon fractions under different land uses on the tableland of the Loess Plateau of China. **Catena**. 115:19-28¸ 2014.
48. LIU D.; WENLIANG J.; JIN X.; LI M.; GUOTING S.; DUAN C.; GUO L.; LIU Y.; ZHAO W.; FANG L. Associated soil aggregate nutrients and controlling factors on aggregate stability in semiarid grassland under different grazing prohibition timeframes. **Science of the total environment**. 777:146104, 2021.
49. LOBATO, F. A. O. et al. Perdas de solo e nutrientes em área de Caatinga decorrente de diferentes alturas pluviométricas. **Agro@mbiente On-line**. v. 3, p. 65-71, 2009.
50. LUCENA R. L.; BORGES DA SILVA F. E.; DE MEDEIROS APRÍGIO T. R.; BEZERRA CABRAL JÚNIOR J. The Influence of Altitude on the Climate of Semiarid Areas: Contributions to Conservation. **The International Journal of Climate Change: Impacts and Responses.** 14:81-93, 2022. DOI: https://doi.org/10.18848/1835-7156/cgp/v14i02/81-93
51. MADRID L.; ARAMBARRI P. Adsorption of phosphate by two iron oxides in relation to their porosity. **Journal of Soil Science.** 36:523-30, 1985. DOI: 10.1111/j.1365-2389.1985.tb00355.x
52. MAIA, S. M. F.; XAVIER, F. A. da S.; OLIVEIRA, T. S. de; MENDONÇA, E. de S.; FILHO, J. A. de A. Impactos De Sistemas Agroflorestais E Convencional Sobre A Qualidade Do Solo No Semi-Árido Cearense. **Revista Árvore**, v. 30, n. 5, p. 837–848, 2006.
53. MARCOLAN, A. L.; ANGHINONI, I. Atributos físicos de um Argissolo e um Latossolo Vermelho sob diferentes sistemas de manejo. **Pesquisa Agropecuária Brasileira**. 2006; 40:1135-1139.
54. MARENGO J. Vulnerabilidade, impactos e adaptação à mudança do clima no setor agropecuário e solos agrícolas. **Parcerias Estratégicas**. 2008:149-75
55. MEDEIROS A. S.; GONZAGA G. B. M.; SILVA T. S.; BARRETO B. S.; dos SANTOS T. C.; MELO P. L. A.; GOMES T. C. A.; MAIA S. M. F. Changes in soil organic carbon and soil aggregation due to deforestation for smallholder management in the Brazilian semi-arid region. **Geoderma Regional**. 33:1-12, 2023. DOI: 10.1016/j.geodrs.2023.e00647
56. MENEZES R., SAMPAIO E., GIONGO V., PÉREZ-MARIN A. Biogeochemical cycling in terrestrial ecosystems of the Caatinga Biome. **Brazilian Journal of Biology**. 72:643-53, 2012. DOI: https://doi.org/10.1590/S1519-69842012000400004
57. OLSON K. R.; AL-KAISI M.; LAL R.; CIHACEK L. Impact of soil erosion on soil organic carbon stocks**. Journal of Soil and Water Conservation**. 71:61A-67A, 2016. DOI: 10.2489/jswc.71.3.61A
58. PALÁCIO H. A. Q.; RIBEIRO FILHO J. C.; dos SANTOS J. C. N.; de ANDRADE E. M.; BRASIL J. B. Effective precipitation, soil loss and plant cover systems in the caatinga biome, Brazil. **Revista Caatinga**. 29:956-965, 2016. DOI: 10.1590/1983-21252016v29n421rc
59. PEREIRA M. G.; LOSS A.; BATISTA I.; MELO T. R. DE; SILVA E. C. DA; PINTO L. A. DA S. R. Biogenic and physicogenic aggregates: formation pathways, assessment techniques, and influence on soil properties. **Revista Brasileira de Ciência Do Solo**. 45:1-23, 2021. DOI: 10.36783/18069657rbcs20210108
60. PINHEIRO JUNIOR C. R.; SALVADOR C. A.; TAVARES T. R.; ABREU M. C.; FAGUNDES, H. S.; ALMEIDA W.S.; SILVA NETO E. C.; ANJOS L. H. C.; PEREIRA M. G. Lithic soils in the semi-arid region of Brazil: edaphic characterization and susceptibility to erosion. **Journal of Arid Land**.; 14:56-69, 2002. DOI: 10.1007/s40333-022-0002-3

61. PRINCE S., VON MALTITZ G., ZHANG F., BYERNE K., DRISCOLL C., ESHELL G., KUST G., MARTÍNEZ-GARCIA C., METZGER J. P., MIDGLEY G., MORENO-MATEOS D., SGHAIER M., THWIN S. Status and trends of land degradation and restoration and associated changes in biodiversity and ecosystem functions. In: MONTANARELLA L., SCHOLES R., BRAINICH A., editors. Assessment Report on Land Degradation and Restoration. **Bonn: Secretariat of the Intergovernmental Science-Policy Platform on Biodiversity and Ecosystem Services**; 2018. p. 221-338.
62. QUEIROZ L. P.; CARDOSO D.; FERNANDES M. F.; MORO M. F. Diversity and Evolution of Flowering Plants of the Caatinga Domain. In: SILVA J. M. C.; LEAL I. R.; TABARELLI M., editors. Caatinga: The Largest Tropical Dry Forest Region in South America: The Largest Tropical Dry Forest Region in South America. **Springer**. p. 23-63, 2018.
63. QUÉNARD L., SAMOUËLIAN A.; LAROCHE B.; CORNU S. Lessivage as a major process of soil formation: A revisitation of existing data. **Geoderma**. 167–168, 135–147, 2011. DOI: 10.1016/j.geoderma.2011.07.031
64. ROWLEY M. C.; GRAND S.; VERRECCHIA É. P. Calcium-mediated stabilisation of soil organic carbon. **Biogeochemistry**. 137:27-49, 2018. DOI: 10.1007/s10533-017-0410-1
65. RÜCKAMP D.; AMELUNG W.; THEISZ N.; BANDEIRA A. G.; MARTIUS C. Phosphorus forms in Brazilian termite nests and soils: Relevance of feeding guild and ecosystems. **Geoderma**. 155:269-79, 2010. DOI: 10.1016/j.geoderma.2009.12.010
66. SALTON, J. C.; MIELNICZUK, J.; BAYER, C.; BOENI, M.; CONCEIÇÃO, P. C.; FABRÍCIO, A. C.; MACEDO, M. C. M.; BROCH, D. L. Agregação E Estabilidade De Agregados Do Solo Em Sistemas Agropecuários Em Mato Grosso Do Sul. **Revista Brasileira de Ciência do Solo**, v. 32, p. 11–21, 2008. DOI: 10.1590/S0100-06832008000100002
67. SAMPAIO Y. S. B. Impactos Ambientais da Agricultura no Processo de Desertificação no Nordeste do Brasil. **Revista de Geografia (Recife)**. 22:90-112, 2008.
68. SANTANA M. O. Atlas das áreas susceptíveis à desertificação do Brasil. Brasília: **Ministério do Meio Ambiente**; 2007.
69. SANTOS H. G.; CARVALHO-JÚNIOR W.; DART R. O.; ÁGLIO M. L. D.; SOUSA J. S.; PARES J. G.; FONTANA A.; MARTINS A. L. S.; OLIVEIRA A. P. O. **O novo mapa de solos do Brasil: legenda atualizada**. Embrapa. 67, 2011.
70. SANTOS H. G. S.; JACOMINE P. K.; ANJOS L. H. C.; OLIVEIRA V. A.; LUMBRERAS J. F.; COELHO M. R.; ALMEIDA J. A.; ARAÚJO FILHO J. C.; OLIVEIRA J. B.; CUNHA T. J. F. **Sistema brasileiro de classificação de solos**. 5ª Ed. Brasília: Embrapa, 2018.
71. SANTOS J. C. N.; DE ANDRADE E. M.; GUERREIRO M. J. S.; MEDEIROS P. H. A.; DE QUEIROZ PALÁCIO H. A.; DE ARAÚJO NETO J. R. Effect of dry spells and soil cracking on runoff generation in a semiarid micro watershed under land use change. **Journal of Hydrology.** 541:1057-66, 2016. DOI: 10.1016/j.jhydrol.2016.08.016
72. SANTOS J. C. N; DE ANDRADE E. M.; PALÁCIO H. A. D. Q.; NETO J. R. D. A.; FILHO J. C. R. Erosive process control in the Brazilian semiarid region. **Revista Caatinga**. 31:695-703, 2018. DOI: https://doi.org/10.1590/1983-21252018v31n319rc
73. SANTOS J. C. N.; PALÁCIO H. A. DE Q.; DE ANDRADE E. M.; MEIRELES A. C. M.; NETO JR DE A. Runoff and soil and nutrient losses in semiarid uncultivated fields. **Revista Ciencia Agronomica**. 42:813-20, 2011. DOI: 10.1590/s1806-66902011000300030
74. SARCINELLI T.S.; SCHAEFER C.E.G.R.; LYNCH L. de S.; ARATO H.D.; VIANA J.H.M.; ALBUQUERQUE FILHO, M.R; GONÇALVES T.T. Chemical, physical and micromorphological properties of termite mounds and adjacent soils along a toposequence in Zona da Mata, Minas Gerais State, Brazil. **Catena.** n. 76, p. 107–113, 2009. DOI: 10.1016/j.catena.2008.10.001
75. SCHAEFER C. E. G. R. Brazilian latosols and their B horizon microstructure as long-term biotic constructs. **Australian Journal of Soil Research**. 39:909-26, 2001. DOI: 10.1071/SR00093
76. SHI P.; ARTER C.; LIU X.; KELLER M.; SCHULIN R. Soil aggregate stability and size-selective sediment transport with surface runoff as affected by organic residue amendment. **Science of the Total Environment**. 607-608:95-102, 2017. DOI: 10.1016/j.scitotenv.2017.07.008
77. SILVA, P. L. F.; OLIVEIRA, F. P.; MARTINS, A. F.; TAVARES, D. D.; AMARAL, A. J. Fertility, carbon stock and aggregate stability of an Alfisol under integrated farming systems. **Pesquisa Agropecuaria Tropical**. 51:1-9, 2021.
78. SIX J.; BOSSUYT H.; DEGRYZE S.; DENEF K. A history of research on the link between (micro)aggregates, soil biota, and soil organic matter dynamics. **Soil and Tillage Research**, 79:7-31, 2004. DOI: 10.1016/j.still.2004.03.008
79. SIX J.; JASTROW J. D. Organic Matter Turnover. In: Lal R., editor. **Encyclopedia of Soil Science**. Boca Raton: **Marcel Dekker**, 2002, p. 936–942.
80. SOLLINS P.; KRAMER M. G.; SWANSTON C.; Lajtha K.; FILLEY T.; AUFDENKAMPE A. K.; WAGAI R.; BOWDEN R. D. Sequential density fractionation across soils of contrasting mineralogy: evidence for both microbial- and mineral-controlled soil organic matter stabilization. **Biogeochemistry**, n. 96, p. 209–231, 2009. DOI: 10.1007/s10533-009-9359-z
81. SOUZA B. I. DE; SUERTEGARAY D. M. A.; LIMA E. R. V. Desertificação E Seus Efeitos Na Vegetação E Solos Do Cariri Paraibano. **Mercator**, 8:217-32, 2009. DOI: 10.4215/rm2009.0816.0017
82. SOUZA J.J.L.L.; SOUZA B.I.; XAVIER R.A.; CARDOSO E.C.M.; MEDEIROS J.R.; FONSECA C.F.; SCHAEFER C.E.G.R. Organic carbon rich-soils in the brazilian semiarid region and paleoenvironmental implications. **Catena**, 212, 2002. DOI: 1016/j.catena.2022.106101
83. STOLT M. H.; LINDBO D. L. Soil Organic Matter. Interpretation of Micromorphological Features of Soils and Regoliths. **Elsevier**, p. 369-96, 2010. DOI: 10.1016/B978-0-444-53156-8.00017-9

84. STOOPS, G. **Guidelines for Analysis and Description of Soil and Regolith Thin Sections**. 2ª Ed. Wiley-Blackwell: Hoboken, 2021, 256 p. DOI: 10.2136/guidelinesforanalysis2
85. STOOPS G.; SCHAEFER C. E. G. R. Pedoplasmation. Interpretation of Micromorphological Features of Soils and Regoliths. **Elsevier**, p. 69-79, 2010. DOI: 10.1016/B978-0-444-53156-8.00005-2
86. TEIXEIRA P. C., DONAGEMA G. K., FONTANA A., TEIXEIRA W. G. **Manual de métodos de análise de solo**. 3ª Ed. Brasília, DF: Embrapa, 2017a.
87. TEIXEIRA P. C., DONAGEMA G. K., FONTANA A., TEIXEIRA W. G. **Manual de métodos de análise de solo**. 3ª Ed. Brasília, DF: Embrapa, 2017b.
88. TOTSCHE K. U.; AMELUNG W.; GERZABEK M. H.; GUGGENBERGER G.; KLUMPP E.; KNIEF C.; LEHNDORFF E.; MIKUTTA R.; PETH S.; PRECHTEL A.; RAY N.; KÖGEL-KNABNER I. Microaggregates in soils. **Journal of Plant Nutrition and Soil Science**. 2018a; 181:104-36. DOI: 10.1002/jpln.201600451
89. TRAORÉ S.; OUATTARA K.; ILSTEDT U.; SCHMIDT M.; THIOMBIANO A.; MALMER A.; NYBERG G. Effect of land degradation on carbon and nitrogen pools in two soil types of a semi-arid landscape in West Africa. **Geoderma,** 241-242:330-8, 2015. DOI: 10.1016/j.geoderma.2014.11.027
90. WANG X.; ZHAO X.; ZHANG Z.; YI L.; ZUO L.; WEN Q.; LIU F.; XU J.; HU S.; LIU B. Assessment of soil erosion change and its relationships with land use/cover change in China from the end of the 1980s to 2010. **Catena**.;137:256-68, 2016. DOI: 10.1016/j.catena.2015.10.004
91. WEI Y.; WU X.; XIA J.; SHEN X.; CAI C. Variation of soil aggregation along the weathering gradient: Comparison of grain size distribution under different disruptive forces. **PLoS ONE**, 11, 2016. DOI: https://doi.org/10.1371/journal.pone.0160960
92. WOLKA K.; BIAZIN B.; MARTINSEN V.; MULDER J. Soil and water conservation management on hill slopes in Southwest Ethiopia. I. Effects of soil bunds on surface runoff, erosion and loss of nutrients. **Science of the Total Environment**, 757:142877, 2021.DOI: 10.1016/j.scitotenv.2020.142877
93. WUDDIVIRA M. N., CAMPS-ROACH G. Effects of organic matter and calcium on soil structural stability. **European Journal of Soil Science**, 58:722-7, 2007. DOI: 10.1111/j.1365-2389.2006.00861.x
94. XAVIER R. A. Processos geomorfológicos e evolução da paisagem no semiárido brasileiro. **Revista de Geociências Do Nordeste**, 7:59-69, 2021. DOI: 10.21680/2447-3359.2021v7n1ID20692
95. XAVIER R. A. Processos erosivos superficiais no município de Juazeirinho, Região Semiárida da Paraíba. **Revista de Geociências Do Nordeste**, 2:113-22, 2016. DOI: 10.21680/2447-3359.2016v2n0ID10465
96. XAVIER R. A.; SEABRA V. S.; DAMASCENO J.; DORNELLAS P. C. Mapeamento geomorfológico da bacia do Rio Paraíba (PB) utilizando classificação baseada em objetos. **Acta Geográfica**, 10:139-52, 2016.
97. YEOMANS J. C.; BREMNER J. M. A rapid and precise method for routine determination of organic carbon in soil. **Communications in Soil Science and Plant Analysis**, 19:1467-76, 1988. DOI: https://doi.org/10.1080/00103628809368027
98. YIN Y.; WANG L.; LIANG C.; XI F.; PEI Z.; DU L. Soil Aggregate Stability and Iron and Aluminium Oxide Contents Under Different Fertiliser Treatments in a Long-Term Solar Greenhouse Experiment. **Pedosphere**, 26:760-7, 2016. DOI: 10.1016/S1002-0160(15)60086-8
99. ZHENG W.; MORRIS E. K.; LEHMANN A.; RILLIG M. C. Interplay of soil water repellency, soil aggregation and organic carbon. A meta-analysis. **Geoderma**, v. 283, p. 39-47, 2016. DOI: 10.1016/j.geoderma.2016.07.025

This work is licenced under the Creative Commons Atribution 4.0 International (http://creativecommons.org/licenses/by/4.0/) – CC BY. This licence allows others to distribute, remix, adapt and create from your work, even for commercial purposes, as long as they give you due credit for original creation.